

# **Doppler Radar for Biomedical Measurements**

April 20<sup>th</sup>, 2004

## **A THESIS**

Submitted to the faculty of the  
Electrical Engineering Department  
Of New Mexico Tech  
in partial fulfillment of the requirements for the course  
EE 482/482L – Senior Design Project

## **BY**

Senior Design Team 4

Aghavni Ball

Derek Lamppa

Nicolas Marrero

Robert Selina

Katsuya Sugimoto



**ABSTRACT**

The Doppler Radar for Biomedical Measurements Project is sponsored by BIOPAC Systems, a medical research equipment manufacturer. They requested that the Electrical Engineering design team modify a preexisting radar prototype to extract a subject's respiration and heart rate from a distance without making contact with the patient. After discussion with the customer, Senior Design Team 4 decided to focus on developing the prototype towards apnea studies. The system consists of a two-antenna continuous wave radar array that receives raw data and transfers it to a signal processing system that consists of adaptive bandpass filters that extract the heart rate and respiration signals from the reflected data signal. Movement in the signal is also identified in addition to identifying the patient's respiration rate, heart rate and apnea specific data including apnea episodes per hour and per session. This is done with a Matlab-generated GUI.

## ACKNOWLEDGMENTS

The authors would like to sincerely thank the following for their assistance and support throughout the project:

Dr. Robert Bond

Dr. Ali El-Osery

Alan Macy

Chris Patscheck

Chris Pauli

Betty Scott

Dr. Chip Scott

Dr. Scott Teare

Carol Teel

Andrew Tubesing

In addition we would like to thank MiniCircuits ([www.minicircuits.com](http://www.minicircuits.com)) and Mouser Electronics ([www.mouser.com](http://www.mouser.com)) for providing hardware samples and reliability information.

# 1 TABLE OF CONTENTS

1	TABLE OF CONTENTS .....	3
2	LIST OF TABLES .....	4
3	LIST OF FIGURES .....	4
4	LIST OF ABBREVIATIONS AND DEFINITIONS (AB) .....	5
5	Introduction (RS) .....	6
5.1	Vital Sign Monitoring and Apnea .....	6
5.1.1	Description of Apnea (DL) .....	6
5.1.2	Apnea Studies (AB) .....	6
6	Background Information on Doppler Radar Applied to Apnea Studies .....	8
6.1	Doppler Radar .....	8
6.1.1	Radar Equation (RS) .....	8
6.1.2	Doppler Frequency and Phase Shift (RS) .....	8
6.2	Technical Contributions to Prototype (AB) .....	9
7	Apnea and Vital Signs Monitoring Subsystems .....	10
7.1	Antenna Array (AB) .....	10
7.1.1	Transmitted and Received Signals (RS) .....	11
7.1.2	Power Density Transmitted (KS) .....	13
7.1.3	Reflected Energy (KS) .....	14
7.1.4	Safety of Radiation (AB) .....	15
7.1.5	Radar Reliability (RS) .....	17
7.2	Radar Data Acquisition and Signal Processing (NM) .....	18
7.2.1	The MP100 and AcqKnowledge (NM) .....	18
7.2.2	Matlab and Algorithms (NM) .....	19
7.2.3	Dataviewer (NM) .....	20
7.2.4	Respiration (DL) .....	23
7.2.5	Heart Rate (DL) .....	27
7.2.6	Movement Algorithm (DL) .....	30
7.2.7	Apnea Episodes (RS) .....	33
7.3	GUI Overview - Data Display and Manipulation (NM) .....	35
8	Recommendations for Future Work (RS) .....	40
9	APPENDICES .....	42
9.1	Appendix A - References .....	43
9.2	Appendix B – Budget (AB) .....	45
9.3	Appendix C - Project Timeline (DL) .....	47
9.4	Appendix D - Reflection and Absorption Supporting Calculations (KS) .....	49
9.5	Appendix E - Permittivity and Conductivity of Biological Tissue as a Function of Frequency ...	51
9.6	Appendix F - Interactions of RF Energy and Biological Tissues (DL) .....	53
9.7	Appendix G - Breakdown of the Major Radar Front-End Components (KS) .....	58
9.8	Appendix H – Radar Evaluation and Design (KS) .....	60
9.9	Digital Appendices .....	66

## 2 LIST OF TABLES

Table 1 - Component by Component Failure Data.....	17
--	----

## 3 LIST OF FIGURES

Figure 1 - Sleep Study Patient in Full Gear.....	7
Figure 2 - Test Setup.....	10
Figure 3 - Block Diagram for 2.4GHz Radar.....	11
Figure 4 - IEEE Standards for Frequency of Transmission.....	16
Figure 5 - Sample Screenshot of the Dataviewer.....	21
Figure 6 - Control Respiration (Black) vs. Radar Signal (Red).....	24
Figure 7 - Sample Radar Magnitude Response for a 10-second Window.....	25
Figure 8 - Original Radar (Blue) with Extracted Respiration (Purple).....	27
Figure 9 - Control Pulse in Time (left) and Frequency Magnitude Response (right).....	28
Figure 10 - Resulting Pulse signal extracted from radar (Black) Against Control Pulse Sensor (Red).....	30
Figure 11 - Data Collection Interrupted by Subject Movement.....	31
Figure 12 - Apnea Episode from Control Sensor and Radar Signal.....	33
Figure 13 - Standard Windows Menu Interface in the GUI.....	35
Figure 14 - Patient Information Dialog Box.....	36
Figure 15 - A Screenshot of the GUI.....	36
Figure 16 - An Example of User Oversight.....	38
Figure 17 - Skin Depth as a Function of Frequency.....	56
Figure 18 - LO Circuit Equivalence.....	58
Figure 19 - Fundamental Oscillator Circuit Representation.....	59
Figure 20 - VCO Representation.....	59
Figure 21 - Phase Noise Diagram.....	64

## 4 LIST OF ABBREVIATIONS AND DEFINITIONS (AB)

**ISM Band** – Industrial, scientific and medical radio frequency bands.

**Apnea** – The cessation of breathing for more than 10 seconds during sleep.

**Hypopnea** – Slow, light breathing during sleep.

**Pulse Plethysmograph** – Sensor that detects changes in blood density to determine pulse rate.

**AHI** – Apnea-Hypopnea Index. A measure of how many apnea episodes occur in one hour. An AHI of five (five episodes per hour) is defined as minor sleep apnea, while cases with anywhere from 15-20 episodes an hour are defined as significant and pathological; this is the cutoff line, above which treatment is recommended.

**Polysomnography** – Most reliable method of diagnosing apnea. It considers brain activity, chest movement and heart rate, eye and jaw muscle movement, leg movement, airflow and oxygen saturation.

**Dataviewer** – Team-generated tool for visual manipulation of datasets.

**GUI** – Graphical User Interface.

**DSP** – Digital Signal Processing.

**VCO** – Voltage Controlled Oscillator

## **5 Introduction (RS)**

The purpose of this project is to use a RF device to monitor a subject's heart rate and respiration without making physical contact. This will be accomplished using continuous wave Doppler radar antennas and data post processing in Matlab to extract the vital signs. The subject's movement and apnea episodes are also monitored and displayed on the Matlab GUI.

### **5.1 Vital Sign Monitoring and Apnea**

#### **5.1.1 Description of Apnea (DL)**

Sleep Apnea (also referred to as Sleep-Disordered Breathing [SDB]) [2] affects approximately 6% to 7% of the American population, about 18 million. An episode of apnea, regardless of nomenclature, is defined as the cessation of breathing for ten or more seconds. Depending on the severity of apnea in a given patient, there may be anywhere from five episodes of apnea in an hour to hundreds of episodes in a night. The number of apnea episodes in an hour is referred to as the Apnea-Hypopnea Index (AHI) [3].

#### **5.1.2 Apnea Studies (AB)**

The most expensive and reliable method of diagnosing the severity of apnea is found at sleep clinics and is known as polysomnography. It is considered the gold standard in determining the seriousness of sleep disorders. Polysomnography uses physiologic sensor leads that monitor brain electrical activity, eye and jaw muscle movement, leg

movement, airflow, respiratory effort (chest movement), heart rate, and oxygen saturation [5]. Video cameras are also used to monitor the patient's body movement throughout the sleep study period. This study, however, requires a large number of sensors directly on the patient to monitor the values of interest. To study the brain's electroencephalogram, six electrodes are needed at certain places on the head. Contact with a multitude of sensors can cause discomfort in the patient and make the results more inaccurate due to changes caused by higher stress levels. The respiration monitor is also a source of uneasiness, as seen below in

Figure 1; It is a sensor that requires a tight, secure fastening around the chest, which is understandably not comfortable.



**Figure 1 - Sleep Study Patient in Full Gear**

The specific values of interest that polysomnography collects for sleep apnea research are brain waves, respiration, heart rate, and body movement. While brain waves cannot be monitored without electrodes, it is ideal to find a way to monitor the other three without making physical contact with the patient (in order to reduce stress and collect more “natural” data). The development of such a product is the focus of this project.

## 6 Background Information on Doppler Radar Applied to Apnea Studies

### 6.1 Doppler Radar

#### 6.1.1 Radar Equation (RS)

The Doppler effect is defined as a shift in the frequency of a wave caused by the relative motion of the transmitting source, the reflecting object, or the receiving system. The Doppler effect will influence the data received from the radar in the following ways:

The Doppler Effect, or Doppler shift, can be described mathematically, as follows:

$$f_d = \frac{2v_r}{\lambda} = \frac{2v_r f_o}{C}$$

where the  $v_r$  is the relative velocity of the targets respect to the radar,  $f_o$  is the transmitted frequency,  $\lambda$  is wavelength and C is the velocity of radiation propagation.

#### 6.1.2 Doppler Frequency and Phase Shift (RS)

In this project, any change in frequency will be unreadable due to its small size relative to the carrier frequency. Respiration produces a contraction or expansion of the chest with a velocity of less than 3cm/sec. The heart contracts at a typical rate of 6cm/sec. Inputting this data into the radar equation yields:

$$f_d = \frac{1.03V_r}{\lambda} = \frac{1.03 \times 0.06 \frac{m}{s} \times 2}{0.125 \frac{m}{s}} = \frac{0.1236}{0.125} = 0.9888Hz$$

This Doppler shift will not be identifiable with a conventional VCO which will vary from its center frequency.

Any observable information will be produced by a change in the phase shift between the received and transmitted signals. How this phase shift is readable is shown below:

$$\begin{aligned}
& V_{(t)} \cos \omega_1 t V_{(r)} \cos(\omega_2 t + \phi) \\
&= V_{(t)} V_{(r)} [\cos \omega t \cos \phi - \sin \omega t \sin \phi] \cos \omega t \\
&= V_{(t)} V_{(r)} [\cos^2 \omega t \cos \phi - \sin \omega t \sin \phi \cos \omega t] \\
&= V_{(t)} V_{(r)} \left[ \frac{1}{2} (1 + \cos 2\omega t) \cos \phi - \left\{ \frac{1}{2} \sin(\omega t - \omega t) + \frac{1}{2} \sin(\omega t + \omega t) \right\} \sin \phi \right] \\
&= V_{(t)} V_{(r)} \left[ \frac{1}{2} \cos \phi + \frac{1}{2} \cos 2\omega t \cos \phi - \frac{1}{2} \sin 2\omega t \sin \phi \right] \\
&= \frac{1}{2} V_{(t)} V_{(r)} [\cos \phi + \cos 2\omega t \cos \phi - \sin 2\omega t \sin \phi] \\
&= \frac{1}{2} V_{(t)} V_{(r)} [\cos \phi + \cos 2(2\pi f)t \cos \phi - \sin 2(2\pi f)t \sin \phi]
\end{aligned}$$

Where  $V_{(t)} \cos \omega_1 t$  is the transmitted signal and  $V_{(r)} \cos \omega_2 (\omega_2 t + \phi)$  is the received signal.  $\cos 2(2\pi f)t \cos \phi$  and  $\sin 2(2\pi f)t \sin \phi$  are high frequency terms and are removed by the low pass filter. As a result, only the phase component remains:

$$V = \cos \phi$$

## 6.2 Technical Contributions to Prototype (AB)

Biopac contributed their two functioning radar prototypes and the design of the 2.4GHz radar to the project. They also supplied a copy of their AcqKnowledge data acquisition software and the necessary MP100 acquisition hardware. The 2.4GHz radar design and the AcqKnowledge MP100 system are used in the final prototype.

## 7 Apnea and Vital Signs Monitoring Subsystems

### 7.1 Antenna Array (AB)

Our antenna array consists of two 2.4GHz radars mounted perpendicular to the subject and sixty centimeters apart. They are positioned one meter from the subject. This distance can be increased to two meters, though signal quality is degraded. A photo displaying a test setup is shown below in Figure 2.

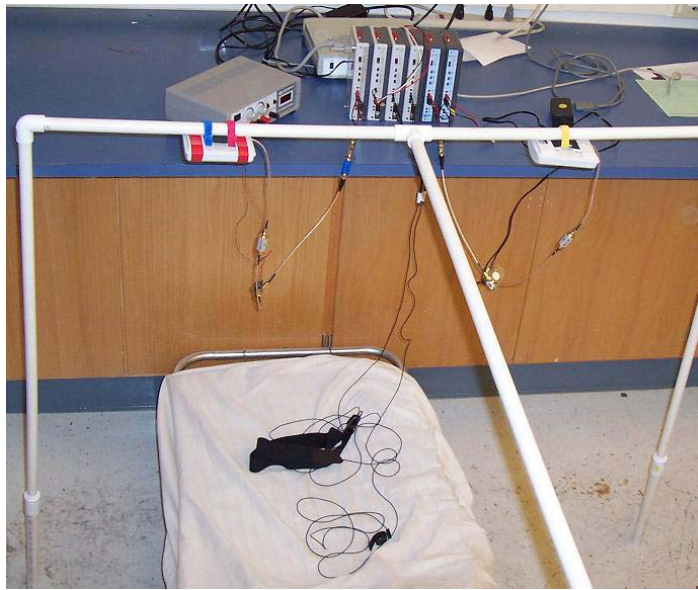


**Figure 2 - Test Setup**

The purpose of two antennas is to be able to have a signal reflected off the back of the subject if they are lying on their side. Data quality is diminished when the subject is lying on their side, but the respiration signal is of a higher magnitude when reflected off the subject's back. Two antennas allow us to collect data in this manner in a wider variety of sleeping positions.

The 2.4GHz radar designed by Dr. Chip Scott for Biopac was never constructed. After testing the prototype 1.85GHz and 900MHz units, a second 900MHz unit and two

2.4GHz units were built to test an array configuration. The 2.4GHz units performed well and were used throughout the project. A block diagram of the 2.4GHz radar units is available below:

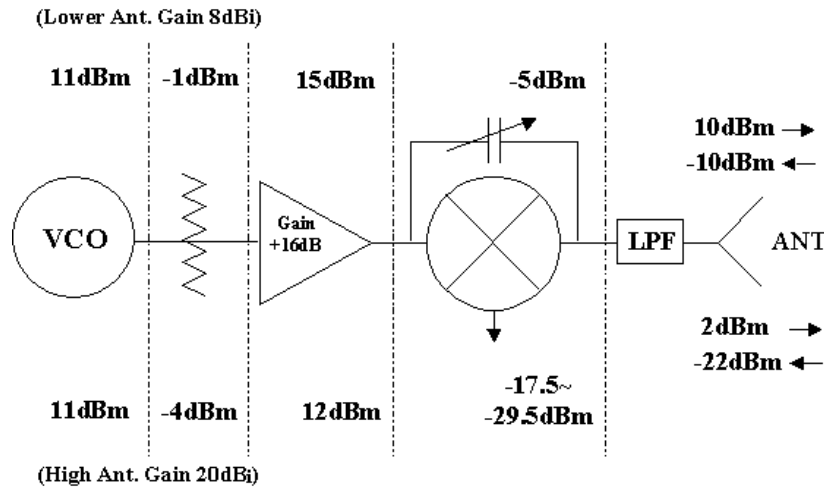


Figure 3 - Block Diagram for 2.4GHz Radar

### 7.1.1 Transmitted and Received Signals (RS)

The radar will transmit a single frequency signal:

$$T(t) = \cos(2\pi ft + \phi(t))$$

where  $f$  is the oscillating frequency and  $\phi(t)$  is the phase drift of the oscillator. The

received signal can be found as:

$$R(t) = \cos \left[ 2\pi f \left( t - \frac{2d \left( t - \frac{d(t)}{c} \right)}{c} \right) + \phi(t) \left( t - \frac{2d \left( t - \frac{d(t)}{c} \right)}{c} \right) \right]$$

where  $c$  is the velocity of propagation and  $d(t)$  is the distance to the target. The signal will be reflected by the target which is at a distance  $d_o$ . The total distance to the target will

also have a time varying displacement component  $x(t)$  which will consist of the vital signs and any other movement. Thus the distance between the transmitter and receiver is  $d(t) = d_o + x(t)$ . After substituting this equality for  $d(t)$ , the received signal becomes:

$$R(t) = \cos \left[ 2\pi f t - \frac{4\pi d_o}{\lambda} - \frac{4\pi x \left( t - \frac{d(t)}{c} \right)}{\lambda} + \phi \left( t - \frac{2d_o}{c} - \frac{2x \left( t - \frac{d(t)}{c} \right)}{c} \right) \right]$$

where  $\lambda = c/f$ . Since the period of oscillation for the vital signs is much larger than  $d_o/c$  and  $x(t) \ll d_o$ , we can approximate the received signal as:

$$R(t) \approx \cos \left[ 2\pi f t - \frac{4\pi d_o}{\lambda} - \frac{4\pi x(t)}{\lambda} + \phi \left( t - \frac{2d_o}{c} \right) \right]$$

The received signal is similar to the transmitted signal with two differences. There is a delay due to the distance  $d_o$  between the transmitter and the target and there is also a phase change due to the periodic motion  $x(t)$ . The mixer multiplies the received signal with the local oscillator signal extracting the changing phase component. The resulting signal can be characterized as:

$$B(t) = \cos \left[ \theta + \frac{4\pi x(t)}{\lambda} + \Delta\phi(t) \right]$$

where:

$$\Delta\phi(t) = \phi(t) - \phi\left(t - \frac{2d_o}{c}\right)$$

is the constant phase shift related to  $d_o$  and:

$$\theta = \frac{4\pi d_o}{\lambda} + \theta_o$$

is the changing phase shift. Thus one can see that the respiration and heart rate signals will be visible on the output of the mixer regardless of the fact that they do not produce a Doppler shift [25].

### 7.1.2 Power Density Transmitted (KS)

Knowing that the vital signs should be present in the received signal, we need to confirm that their magnitudes will be measurable. We determined the power density transmitted by the radar and found that it is the maximum permissible under current ANSI/IEEE regulations.

The power density of the radar is described as follows:

$$\rho = \frac{G_A P_{rad}}{4\pi r^2} = \frac{1}{2} \text{Re}\left\{\hat{\mathbf{E}} \times \hat{\mathbf{H}}^*\right\} \left(\frac{W}{m^2}\right)$$

This can be expanded to:

$$\begin{aligned}\rho_{ave} &= \frac{1}{2} \operatorname{Re}\{\hat{\mathbf{E}} \times \hat{\mathbf{H}}^*\} = \frac{1}{2} \operatorname{Re}\left\{|\hat{\mathbf{E}}|^2 \left(\frac{1}{377}\right) \vec{a}_z\right\} = \frac{1}{2} \operatorname{Re}\left\{|\hat{\mathbf{E}}_{m1}^+(-0.72 - 0.034j)|^2 \left(\frac{1}{377}\right) \vec{a}_z\right\} \\ &= \frac{1}{2} (\hat{\mathbf{E}}_{m1}^+(-0.72))^2 \left(\frac{1}{377}\right) = 6.875 \times 10^{-4} (\hat{\mathbf{E}}_{m1}^+)^2 (W/m^2)\end{aligned}$$

Where the intrinsic impedance of free space is:

$$\hat{\eta}_1 = \frac{|\hat{\mathbf{E}}|}{|\hat{\mathbf{H}}|} \Rightarrow |\hat{\mathbf{H}}| = \frac{1}{377} |\hat{\mathbf{E}}|$$

The transmitted wave from our antenna  $\hat{\mathbf{E}}_{m1}^+$  is left as notation in this calculation because  $\hat{\mathbf{E}}_{m1}^+$  will vary depending on the antenna gain.

### 7.1.3 Reflected Energy (KS)

It is very important for the radar system to receive enough reflected energy so that it is able to compare the differences between the RF and LO signals. For this reason, the ratio of absorbed and reflected energy must be calculated.

The ratio of the energy that is reflected back from hitting a target is expressed in the following equation.

$$\hat{\mathbf{E}}_{m1}^- = \hat{\mathbf{E}}_{m1}^+ \left( \frac{\hat{\eta}_2 - \hat{\eta}_1}{\hat{\eta}_2 + \hat{\eta}_1} \right)$$

Where  $\hat{\eta}$  is the intrinsic impedance of the objects:

$$\hat{\eta} = \sqrt{\frac{\mu}{\epsilon - j\frac{\sigma}{\omega}}}$$

In this case, the boundary between free space and skin is used. For our research, the parameters such as relative  $\sigma$  (conductivity), relative  $\epsilon$  (permittivity), and relative  $\mu$  (permeability) of human skin are 1.0, 33, and  $4\pi \times 10^{-7}$  respectively.

We obtained the ratio of

$$\hat{E}_{m1}^- = \hat{E}_{m1}^+ (-0.72 - 0.034j)$$

This result shows that around 70 percent of the energy is expected to be reflected back to our radar. Supporting calculations are available in Appendix D.

#### 7.1.4 Safety of Radiation (AB)

Radiation safety issues need to be considered when using radar on a human subject.

Radiation standards are governed by OSHA and standards have been set by IEEE and ANSI. The primary health effect caused by non-ionizing radiation is heating when the subject absorbs the transmitted energy. Prolonged radiation exposure above the OSHA levels can produce adverse health effects. At the operational frequency of 2.4GHz, radiation power density at the subject cannot exceed  $2\text{mW}/\text{cm}^2$  based on the ANSI and IEEE standard. Figure 4 is the IEEE standards of transmission.

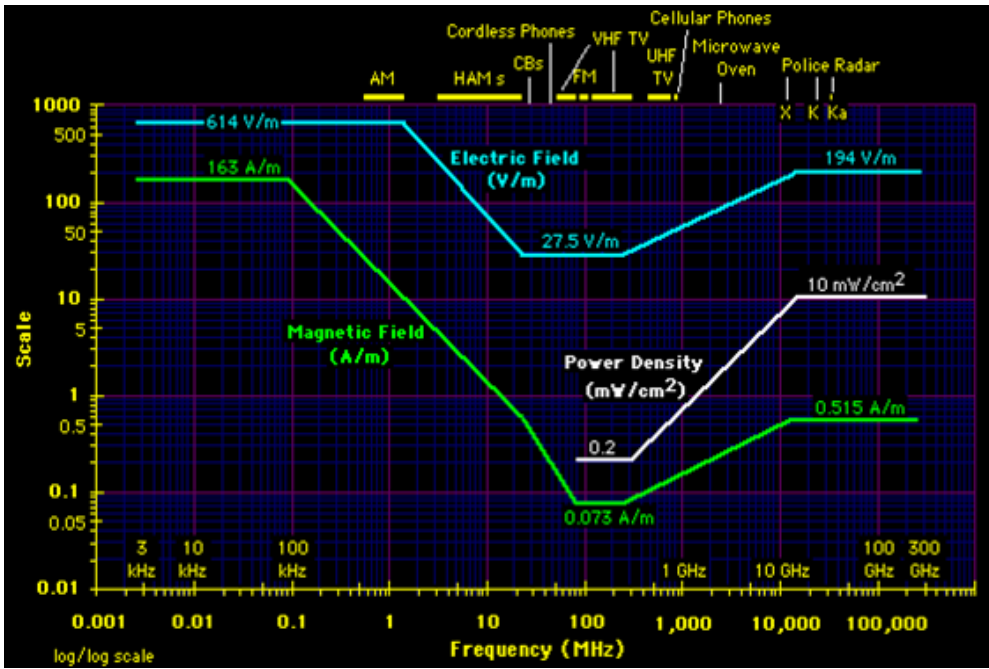


Figure 4 - IEEE Standards for Frequency of Transmission

The power density ( $\rho$ ) at the subject is as follows:

$$\rho = \frac{G_A P_{rad}}{4\pi r^2} = \frac{1}{2} \text{Re} \{ \hat{\mathbf{E}} \times \hat{\mathbf{H}}^* \} \left( \frac{W}{m^2} \right)$$

Inserting values for the above we obtain:

$$\rho = \frac{P_t G_t}{4\pi r^2} \left( \frac{W}{m^2} \right) = (-20 + 8 - (11 + 6.02)) \text{dB} = -29.02 \text{ dB/m}^2 = 0.00125 \text{ w/m}^2$$

The IEEE/ANSI standard is:

$$F = 2 \text{ m w/cm}^2 = 20 \text{ w/m}^2$$

The power density at the target is well below the maximum allowable levels of radiation.

### 7.1.5 Radar Reliability (RS)

The mean time to failure (MTTF) for our two radar-antenna array is 7.07 years. This is based on data obtained from an online component reliability database, <http://www.sercoassurance.com/the-srda/>, and from Minicircuits, the manufacturer of the used IC devices. Table 1 indicates the reliability data for a single radar antenna.

#### Component Failure Analysis

Component	Description	Failure Rate (per year)	MTTF (hours)	Failure Rate (per million hours)
JTOS-3000P	VCO		1887438	0.5298
VNA-25	Amplifier		8760000	0.1142
LAT-12	Attenuator		8760000000	0.0001
ALY-44MH	Mixer		2937784	0.3404
	Variable Capacitor	0.00351		0.4007
	Variable Resistor	0.191		21.8037
	Surface Mount Capacitor	0.00181		0.2066
	Antenna			6.6600
	In-line Terminator (Resistor)	0.00577		0.6587
	BNC to SMA Cables			0.0014
	Power Supply			1.5800
<b>Total Failure Rate: (per million hours)</b>				<b>32.2955</b>
<b>MTTF (Hours):</b>				<b>30964.0412</b>
<b>MTTF (Years):</b>				<b>3.5347</b>

Table 1 - Component by Component Failure Data

The mean time to failure for a single radar unit is 3.53 years. However, since we are using two radar devices that can work independently, the system MTTF is 7.07 years.

The system is redundant because should one device malfunction, the other would still collect valid data.

The MTTF for these designs is lacking, and largely cut short by the failure rate of the variable resistor. There is also a design flaw on the existing prototypes related to this resistor. The potentiometer will short out the power supply when adjusted to zero ohms, since there is no additional resistance in series with the potentiometer to prevent current flow. This causes the monolithic amplifier in the circuit to fail.

## **7.2 Radar Data Acquisition and Signal Processing (NM)**

Our Data Acquisition and Signal Processing System consists of two steps. The data is collected using Biopac's provided MP100 system in real time and then post processed using a team-generated Matlab program (GUI).

### **7.2.1 The MP100 and AcqKnowledge (NM)**

AcqKnowledge and the associated MP100 hardware are used to digitize the data and save it as a text file for future manipulation. AcqKnowledge is Biopac's proprietary data acquisition system and it has more functionality than is required for this application. The Biopac resources are for proof of concept; any future marketable version of this prototype will include a much simpler data acquisition system that lacks almost all of the functions of the AcqKnowledge program.

Regardless of the final program used to sample data, our created processing system requires a text file input consisting of two to four tab-delineated columns, each corresponding to one set of sampled. In the final phase of our product, the input to the Matlab program only consists of the two radar channels in two columns. For data validity verification purposes, heart and respiration control rates can be received as well in the other two channels (columns of data). The input data needs to be consisting of 200 samples a second (200Hz) for accurate analysis in the processing system of the Matlab program.

### **7.2.2 Matlab and Algorithms (NM)**

The data collected using AcqKnowledge is post processed in Matlab. The raw feeds from both radars are received and the following are extracted:

- Heart Rate Signal
- Respiration Rate Signal
- Movement Signal

The numeric heart rate, respiration rate, the magnitude and duration of motion and occurrences of apnea. The Graphical User Interface (GUI) is a final version of a test program written for the project called the Dataviewer.

### 7.2.3 Dataviewer (NM)

For visual manipulation of the data, a user-controllable program called **Dataviewer** was created to test the algorithms written for the project. It has the capability to display any portion of any channel in the time domain, frequency (magnitude) domain, and the phase domain. It also has numerous other functions that will be individually described below. Figure 5 on page 21 shows a screenshot of the Dataviewer.

Datasets are loaded in via the “Load Data From File” button (see Figure 5). The main window of the dataviewer is the graphical display, presenting the data from the selected channel over the window. The window is fully scalable by using the mouse-controlled zoom function inherent in Matlab plots. This allows a user to investigate data in detail. For the time domain, the x-axis is always in terms of seconds, referenced from the start of the data collection, and the y-axis is the voltage of the signal. For the frequency (magnitude) domain, the x-axis is expressed in Hz for ease of recognition of the characteristic signal peaks.

The six checkboxes on the left below the window (labeled ‘Options’) are functions that allow a user to further explore the datasets:

- **Hold Enabled:** Should a user wish to overlay two different channels for a more direction comparison, he should use the Hold function. This holds whatever datasets are currently displayed in the window and plots the next selected dataset over it. This can be repeated indefinitely.

- **Zero Padding:** Adds zero padding to the frequency domain output to produce smoother curves.

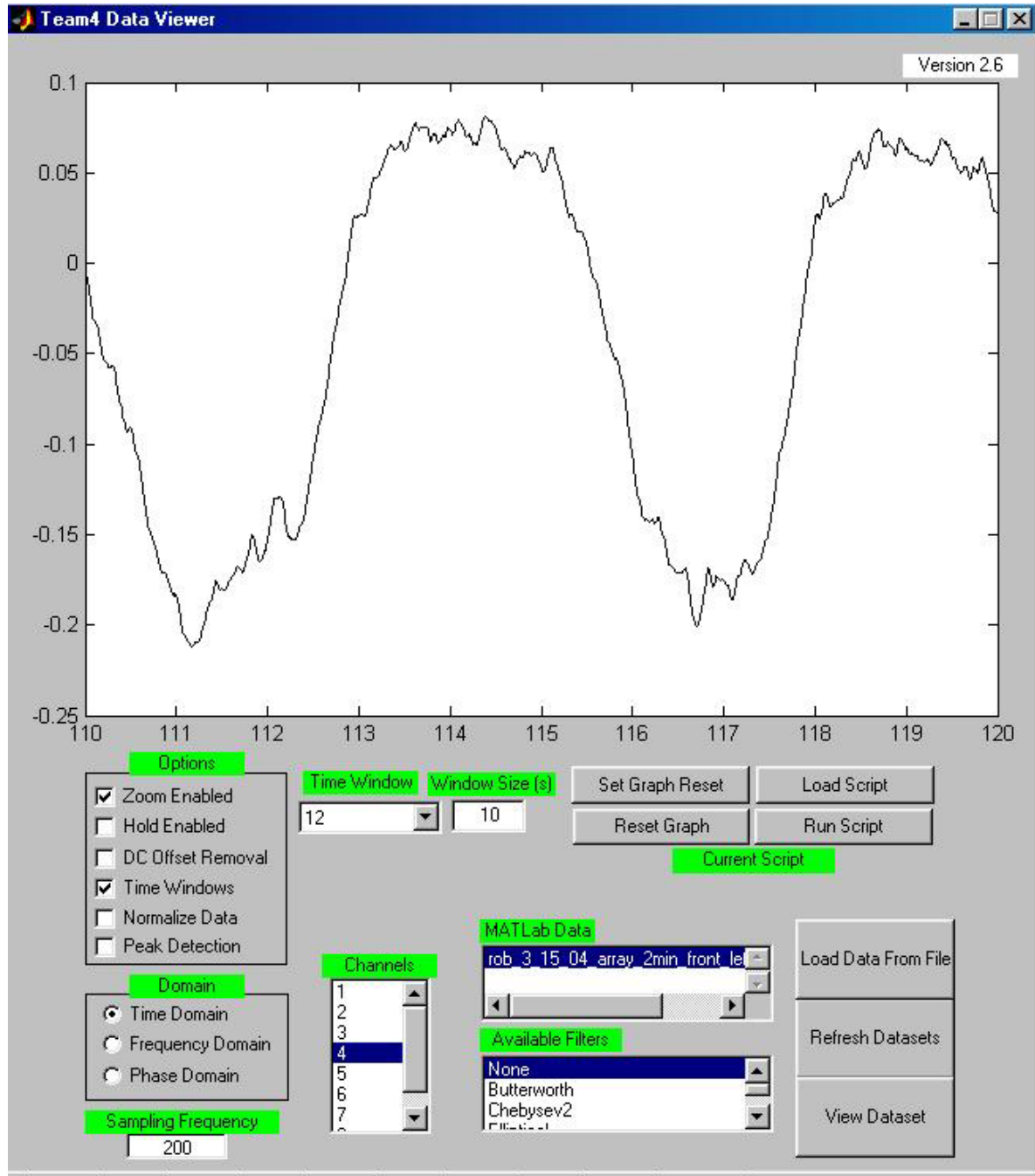


Figure 5 - Sample Screenshot of the Dataviewer

- **DC Offset Removal:** This subtracts from the dataset (or time window) the mean of the set. This removes the DC component, which appears as a large peak at 0 Hz in the Frequency magnitude domain. Removing this large peak makes displaying the rest of the frequency components easier.
- **Time Windows:** This function allows a user to divide the dataset into windows of a user-defined length and select any portion of it for display. This is helpful to simulate the window-by-window data-processing algorithms, and to look at the characteristics of a smaller portion of the data.
- **Normalize Data:** When comparing two sets of data using the hold function, the data can be of different magnitudes. Using this function, one can define the normalization factor to which the dataset is scaled to, allowing overlapping comparison between datasets.
- **Peak Detection:** This is the peak finding algorithm used in the respiration- and pulse-rate finding algorithms. It analyzes the windowed data and finds the relative peaks throughout, placing a mark on each. This is best used with the hold function on, so that the peaks can be overlaid on the original graph.

Below “Options” is the “Domain” section, which allows a user to select the domain that the plot displays. The sampling frequency below is used to calculate the time and frequency index used in the plots; obviously, data sampled at a frequency of 100 Hz could not be displayed accurately on the same time index as that of a 200 Hz dataset. To the right of that is the channel select, in which a user can choose the channel to be displayed. To the right of the channel select is the filter selection, in which standalone

filter programs can be dropped in and applied to the data. Standard filters, like the Butterworth low pass filter, and special filters, like a manual version of the respiration-rate finding algorithm, are found in here and can be applied to a given dataset.

The “Load Script” and “Run Script” functions allow a user to employ scripts that automatically use all the previously described functions to display a complex product; one such script included with the Dataviewer, CheckRespiration, is an automated version of the respiration-rate finding algorithm, using the Dataviewer functions.

Most of these functions are implemented by the back-end of the GUI automatically. These algorithms are discussed in more detail in the following sections.

#### **7.2.4 Respiration (DL)**

The radar waves pick up a phase shift as they encounter the moving chest cavity; this phase shift is dependent on the relative velocity of the chest when the transmitted wave encounters the boundary of the chest. This phase shift is responsible for the appearance of the respiration rate in the sampled waveforms.

To understand what sort of periodic signal to extract from the sampled radar data, it is helpful to have a reference signal that is the exact respiration signal. To this end, Biopac provided a pressure sensitive sensor that wraps around the chest and creates an output voltage based on the chest cavity movement. Figure 6 shows the use of the Dataviewer to overlay the radar signal over the control respiration signal for a given time window. The red curve is the radar data and the black is the reference signal data.

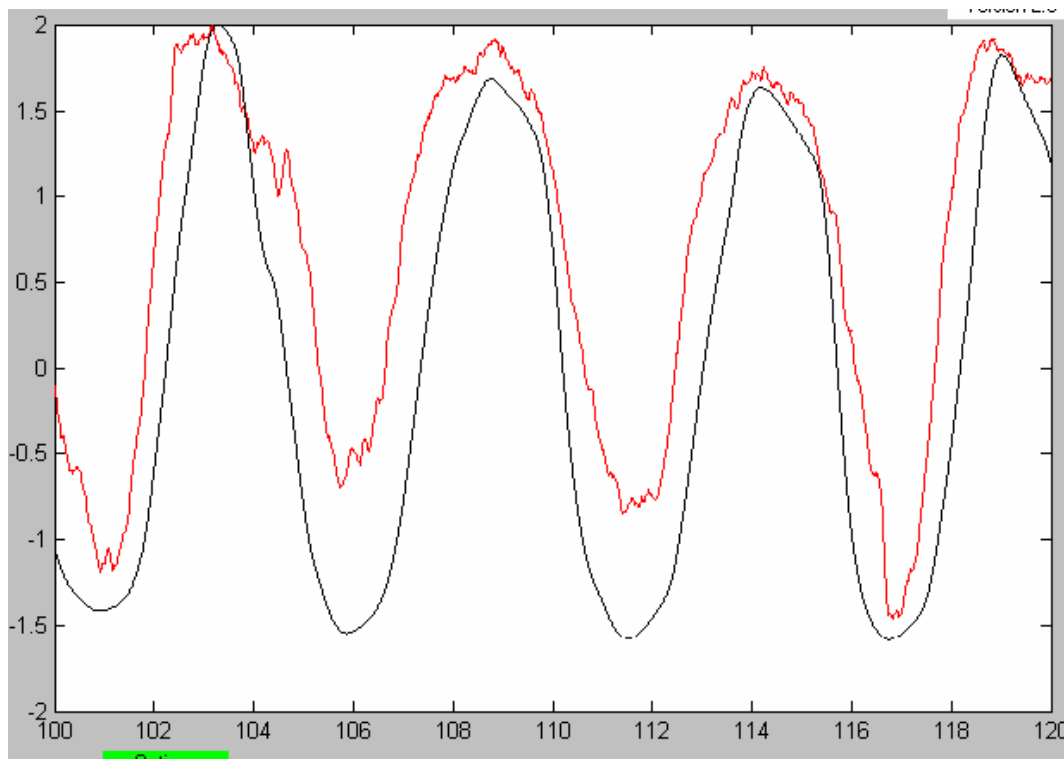


**Figure 6 - Control Respiration (Black) vs. Radar Signal (Red)**

The radar data was normalized for a better visual comparison. Looking at Figure 6, it is clear that the radar carries the respiration rate data. In order to extract the pure waveform, an adaptive bandpass filter was created, which locates the characteristic frequency peak of the respiration in the frequency domain and follows it through time windows that progress through the dataset.

The adaptive bandpass filter begins with, the data being filtered using a low pass filter with a stop band beginning at 3Hz, to remove all noise in the radar greater than the limits of the biological signals (respiration can occur at a rate up to 1.2 Hz, while heart rate is assumed to stay below a 3Hz [180 bpm] rate).

The data is viewed in a ten second window that slides over the data in five-second increments. The time domain data in the window is then run through a process called the

Fast Fourier Transform (FFT), which yields a set of complex numbers containing the frequency, magnitude and phase responses of the data in the time window. The magnitude response is of interest, because it is here that the characteristic frequency peak is found with the peak finding algorithm. Figure 7 shows a sample magnitude response in the frequency domain of an average time window.

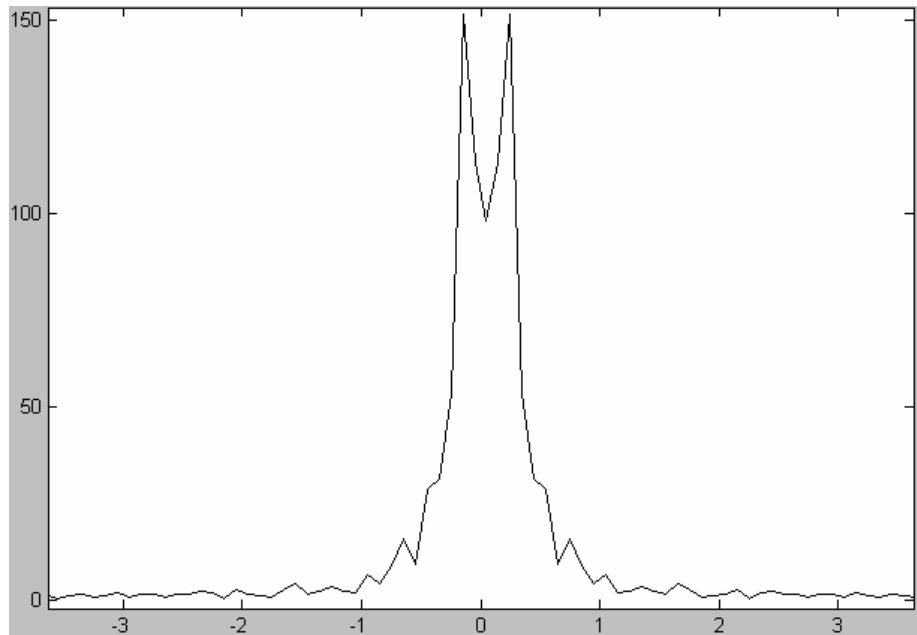


**Figure 7 - Sample Radar Magnitude Response for a 10-second Window**

The DC component has been removed using the DC offset algorithm. The DC bias in the radar data comes from the bleed-through from the LO to the RF input of the mixer on the radar device hardware. This resolution is typical of a ten-second window; for visual purposes, the signal can be zero-padded for higher resolution, but it is clear that the respiration characteristic peaks are visible here. In this time window, these peaks correspond to a respiration rate of approximately 0.2Hz (one breath every five seconds), which is perfectly reasonable for a person at rest.

Because the time window is a rectangular function being applied to a specific portion of the dataset, one may expect to see sidelobe leakage in the frequency domain [22]. This is typically something to be concerned about, and using a Blackman or Hanning window instead of a rectangular window can diminish this effect. However, for the purposes of this project, it is not necessary. There is not significant energy leakage to make these peaks indistinguishable; they are simply too significant to be lost in the leakage.

This characteristic frequency peak is easily found with the peak-finding algorithm. This frequency becomes the center of the bandpass filter, whose transition bands are then placed on the nearest relative minima on either side of the peak. This band of data can then be put back in the time domain via the Inverse Fast Fourier Transform (IFFT) and displayed for each window. The phase shift is still present in the extracted respiration from the radar, but only visible when compared directly to the control respiration signal. By averaging the respiration frequency (the main peak) for the time windows in a given time spread, we can easily determine the respiration rate for a whole dataset or any subset therein.

Figure 8 shows 50 seconds of original radar data, in blue, while the purple waveform is the isolated respiration data. The main frequency component of the respiration signal has been extracted and can be clearly displayed.

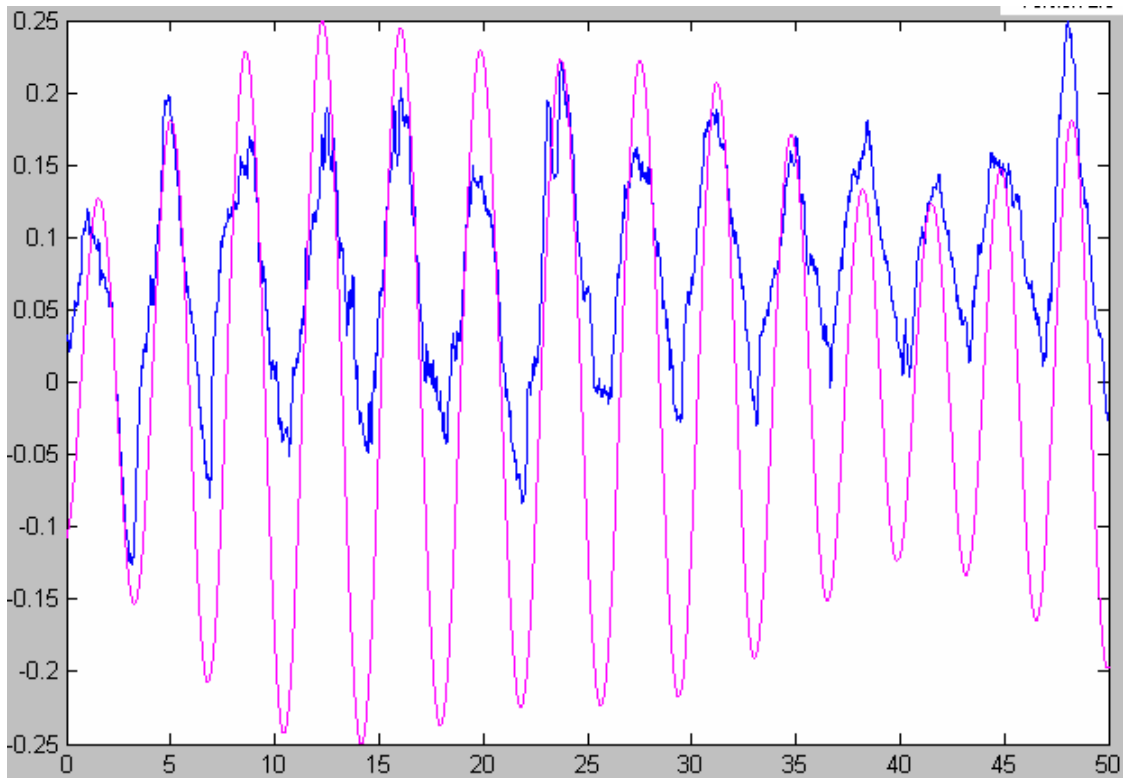


**Figure 8 - Original Radar (Blue) with Extracted Respiration (Purple)**

This algorithm proves to be very robust in finding the respiration from the radar data under all conditions and positions of the body beneath the radar antenna system. When apnea episodes occur in the same time window, the frequency response is not drastically affected; the apnea effects, which appear as noise because respiration stops (leaving only pulse data and system noise). This is effectively zero padding, having minor influence on the magnitude of the very low frequency components.

### **7.2.5 Heart Rate (DL)**

The pulse rate is picked up by the reflection of the RF energy off the periodically varying position of the heart as it beats. Because the radiated energy has numerous boundaries to interact on the approach and return path from the heart (skin, ribs, cartilage, blood, and

fat), and it also is hitting a moving target with smaller total displacement, the returned pulse signal is understandably much smaller than the respiration signal. The respiration amplitude is, on average, one hundred times larger than that of the pulse amplitude. This makes isolating the heart rate more difficult, and a different approach is required. The amplitude of the noise from the system also makes it more difficult to discern the pulse rate from the signal, since the ambient noise is of approximately the same amplitude.

Once again, it is helpful to have a reference signal against which to compare the time-varying reflected waveforms. Biopac provided a sensor for this purpose, one that detects changing densities in blood in the tip of a finger. Figure 9 shows a reference signal response and its characteristic magnitude response in the frequency domain.

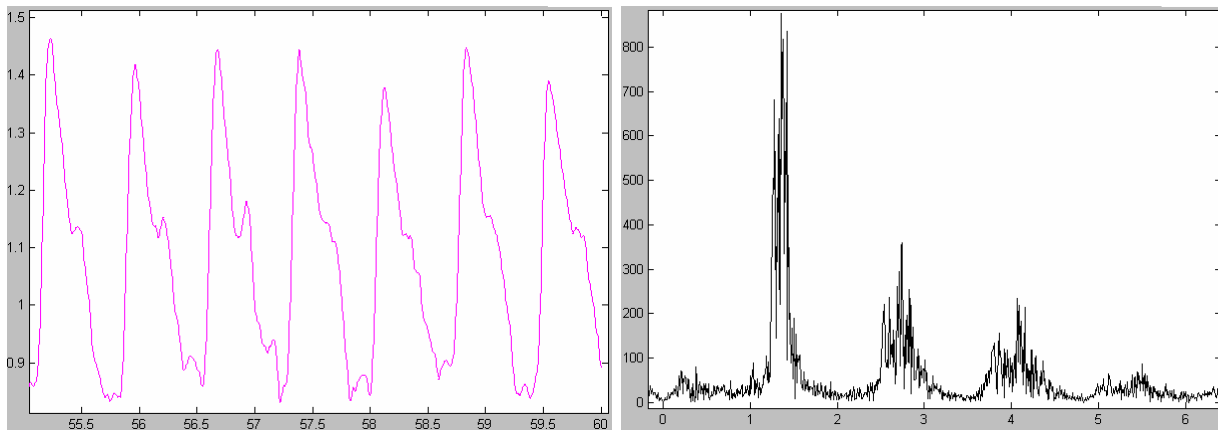


**Figure 9 - Control Pulse in Time (left) and Frequency Magnitude Response (right)**

One expects the pulse signal to appear periodic, and it does. What was unexpected was the harmonic nature of the magnitude response. The first and second harmonics occurring roughly two and three times above the characteristic peak frequency. They appear as a result of the density variances in the blood that the sensor picks up. To extract a similarly appearing pulse signal from the radar, these signals must be

approximated from the radar signal. However, the radar does not pick up these harmonics, and so they will have to be artificially created from the ambient noise occurring at these frequencies. First, though, a general discussion of extracting the pulse signal from the radar follows.

Because the pulse signal is a few orders of magnitude smaller than the respiration signal, the respiration frequency data must be removed before pulse analysis can begin. The lower-frequency, higher-magnitude respiration signal is cut off with a lowpass filter with a stop band up to 1 Hz. The resulting signal then has a lower average amplitude and is fitted for analysis. Next, the positive and negative peaks of the 1 to 3Hz range (relative maxima and minima respectively) are found and tallied. The positive peaks are sorted and the peak ratio (the ratio of one peak's amplitude to the next) is considered. If this peak ratio is greater than 0.5, then the peaks are not far enough apart. The pulse characteristic frequency peak stands above the surrounding noise by about 4 times larger, so that when the highest ratio (differential) is seen, the initial peak is treated as our characteristic frequency peak of the pulse data. Once this peak is located, the two surrounding relative minima become the cutoff bands of the adaptive bandpass filter that follows the main component of the pulse signal. Once again, this signal is IFFTed and displayed in the GUI.

This only reproduces a single sine wave that contains the main frequency component of the pulse (similar to Figure 8, the respiration signal). To generate a signal that looks more like the reference pulse, the harmonics have to be artificially induced. The radar does not pick up the harmonics from the interaction with the movement of the heart, so a technique must be created to simulate their presence. This is done by

multiplying the characteristic frequency bandwidth range by two and three, and amplifying the signal noise held therein. This produces a reasonable approximation of the natural harmonics of the pulse signal and yields the results, as seen in Figure 10.

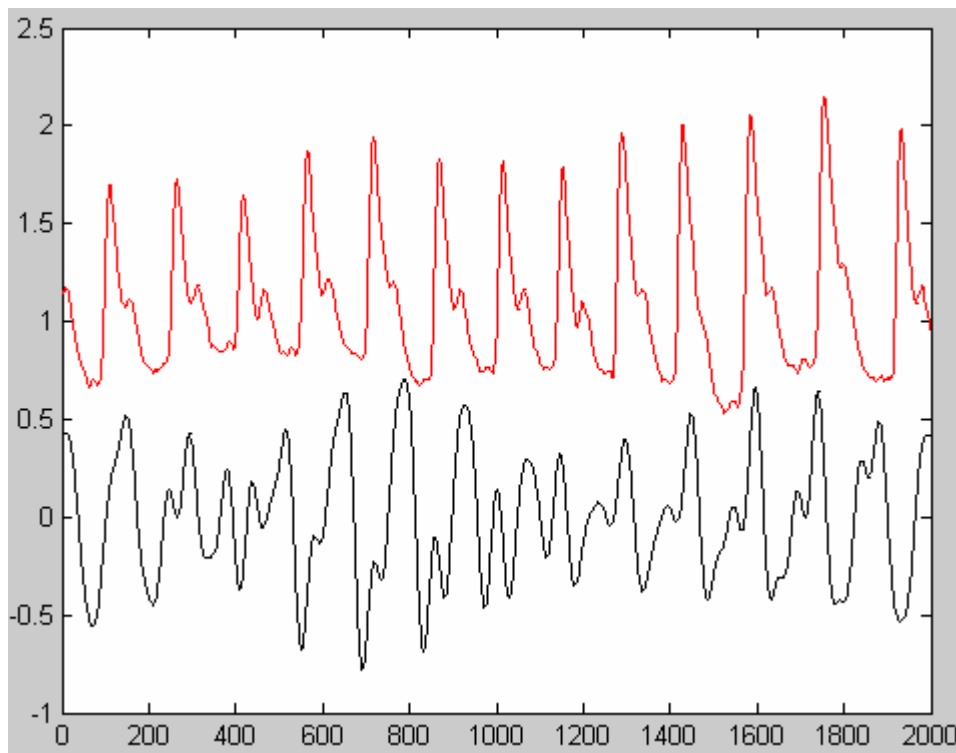


**Figure 10 - Resulting Pulse signal extracted from radar (Black) Against Control Pulse Sensor (Red)**

With these two basic algorithms complete, the project was ready to move into the case-specific design of creating a program for sleep monitoring. To do this, algorithms to detect movement and apnea episodes are required.

### **7.2.6 Movement Algorithm (DL)**

Unfortunately, one aspect of conducting a sleep study on a fully mobile patient is that he or she is just that: fully mobile. Because the patient is not movement-limited by sensor gear or restraints, he is able to exhibit normal movement patterns during sleep. This

movement effectively nullifies the radar data during the movement and for a period afterwards. Figure 11 shows a sample radar waveform that has movement data. When the subject moves, he or she causes abrupt amplitude jumps and uncharacteristic frequency response. Note that after the movement episode, the data does not immediately settle back down into the predictable periodic signal that it used to be. On average, it takes two to three seconds to fully reacquire the respiration and pulse rates.

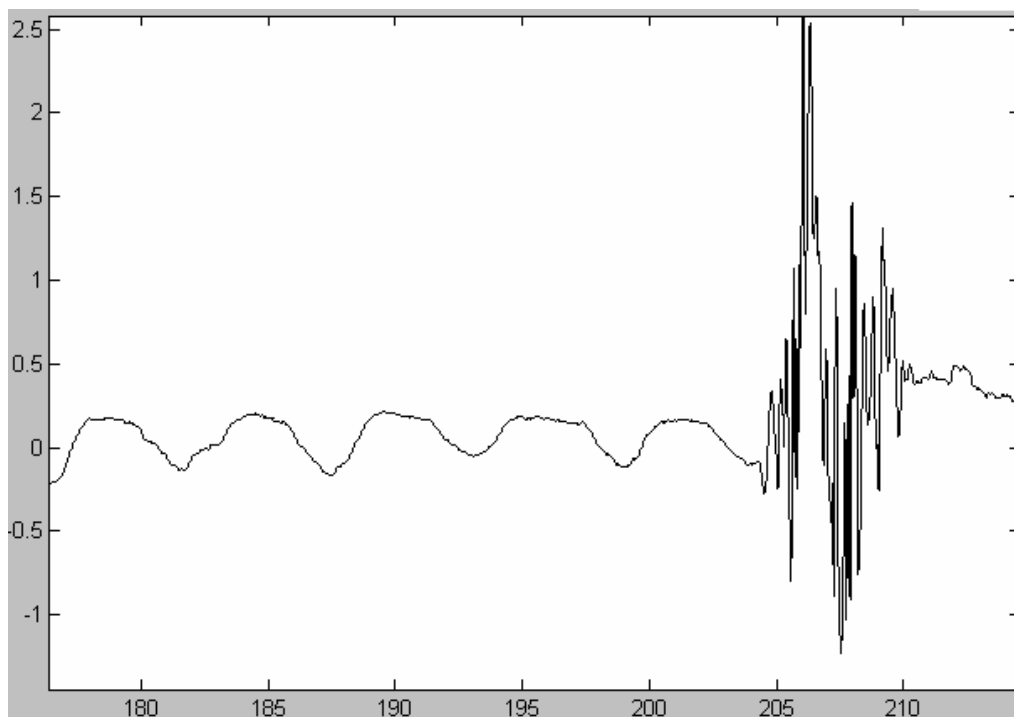


**Figure 11 - Data Collection Interrupted by Subject Movement**

To effectively tally these regions in a collected set of data so that the other algorithms won't consider them, a movement locating algorithm had to be created. This algorithm is to go through the radar datasets and mark sections of the data that are movement. To accomplish this, the function is passed anywhere from a small time window to the whole data set, which parses the passed subset into an  $X$  by 200 matrix, where  $X$  is the number of seconds in the data. The maximum and minimum values for

each second are found and stored. Then, the mean of each second is stored in an array. For any given second, if the maximum or minimum peak is above or below the average by a given threshold, the second is marked as containing movement. The function then tallies the number of seconds in a row that are marked, and outputs the duration of the movement as well as the start of movement (the second it started, based within the data timestamp reference).

The function has a few additions in it to assure robust operation. First, since there may be a case where a second of data is characterized by the downward drop of a periodic signal (which may be outside the governing thresholds), any cases of movement that only last one second are disregarded. Also, if in the middle of a string of seconds of movement, should one second inside the string not meet the criteria to be considered movement, it is assumed to be inside a longer string of movement. For example, should 2 seconds of movement and 3 seconds of movement be separated by one second that does not register as movement, they are all output as one six-second episode of movement.

The output is sent to the GUI, which isolates these ranges from the radar data and displays them in the movement channel of the GUI. The GUI backend also makes note of these ranges for use by the other algorithms, which disregard them in their processes.

### 7.2.7 Apnea Episodes (RS)

In the radar signal data set, an apnea episode is characterized by the disappearance of the respiration signal for a ten-second interval. As a result, the amplitude variations of the radar drop significantly and the signal is reduced to the heart rate and the system noise.

Figure 12 shows the control respiration sensor picking up an apnea event (red), while the black curve is the raw radar data feed. The apnea episode occurs between 30 and 40 seconds.

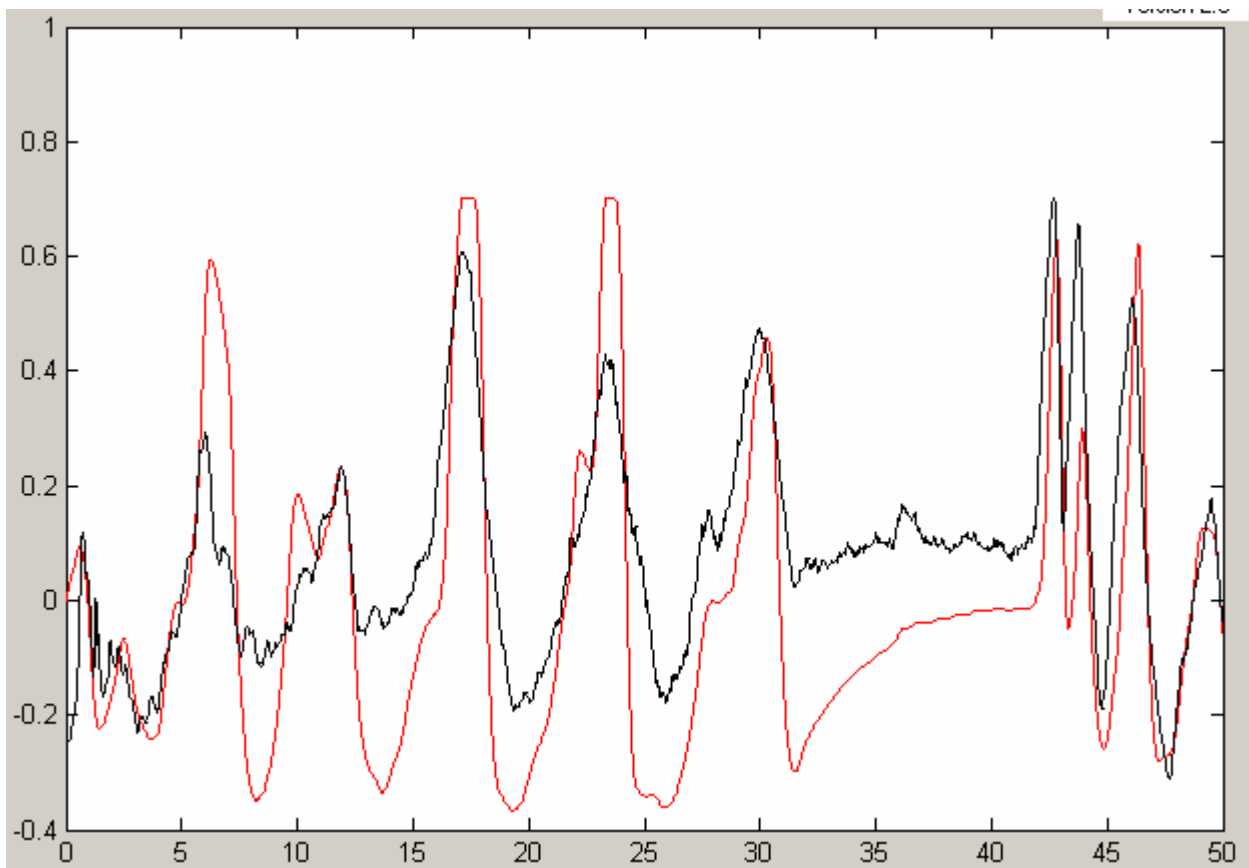


Figure 12 - Apnea Episode from Control Sensor and Radar Signal

Since the large signal of the respiration has disappeared, the radar signal only varies by fractions of what it once did. As a result, a modification of the movement algorithm can be used to determine the starting time and duration of apnea episodes. The beginning of the algorithm is still the same; the signal is partitioned into one second increments and analyzed. The average value, maximum, and minimum peaks for each second increment are also found.

Similar to the movement algorithm, the average value and the maximum and minimum peaks are compared, but for the case of apnea, the peaks must be within a certain bandwidth threshold. That is, if a given second has both its maximum and minimum peaks within 0.1 of the average value for the second, it is safe to conclude that there is no respiration component present and that it may be part of an apnea episode (thus raising a flag for the second). Using the tallying system of the movement algorithm, if ten or more consecutive seconds occur with raised flags, then the time set is considered to be an episode of apnea. It is considered as such until two consecutive seconds have lowered flags; then the apnea episode has a beginning time index, length, and an ending time index.

Once a dataset has been analyzed in this manner, the total number of episodes are counted up and divided by the total length of the data set in hours. This number is then displayed in the GUI as the Apnea-Hypopnea Index (AHI). This is the tell-all signifier that indicates whether or not a patient has a diagnosable level of sleep apnea.

### 7.3 GUI Overview - Data Display and Manipulation (NM)

The GUI serves as an interface between the user and the algorithms developed to extract signals from the radar data. From the standard Windows interface menus (Figure 13), the user can load a saved data set, save a processed data set, close the current data set, print the current data set, exit the program, modify patient information, modify the data display axes, obtain help on using the GUI, obtain version information about the GUI, or put the GUI in a special operating mode called Debug Mode.

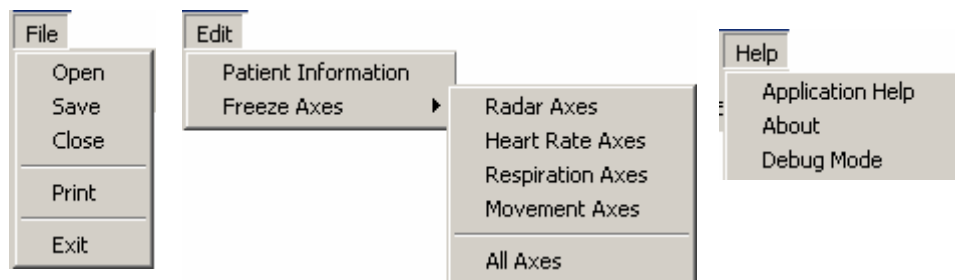


Figure 13 - Standard Windows Menu Interface in the GUI

When a user loads a data set, the GUI asks for the patient's name, date of collection, and collection start time, as shown in the dialog in Figure 14. It then processes the data by sending it out to the Respiration, Heart Rate, Movement, and Apnea algorithms and stores the returned data, presenting it to the user. The user can then scroll through the data using the mouse or using the *Jump To Time Index* box, as shown in Figure 15.

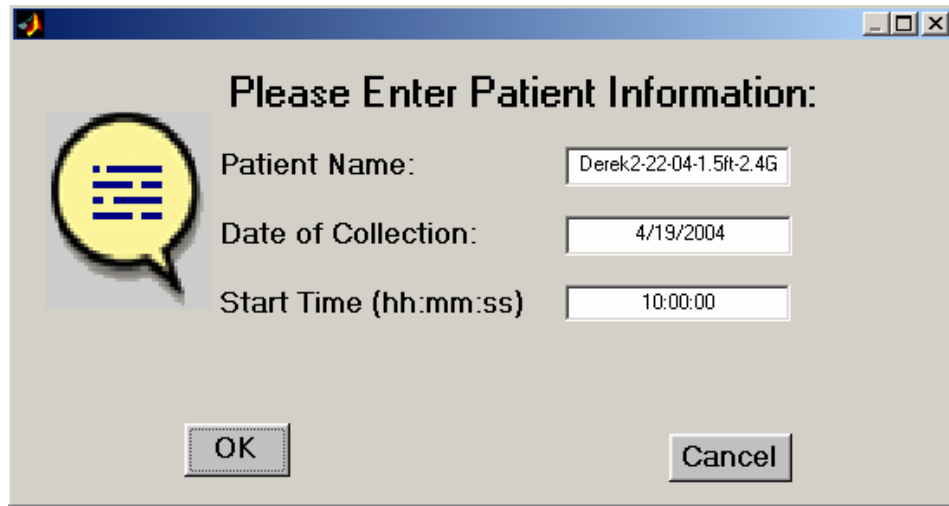


Figure 14 - Patient Information Dialog Box

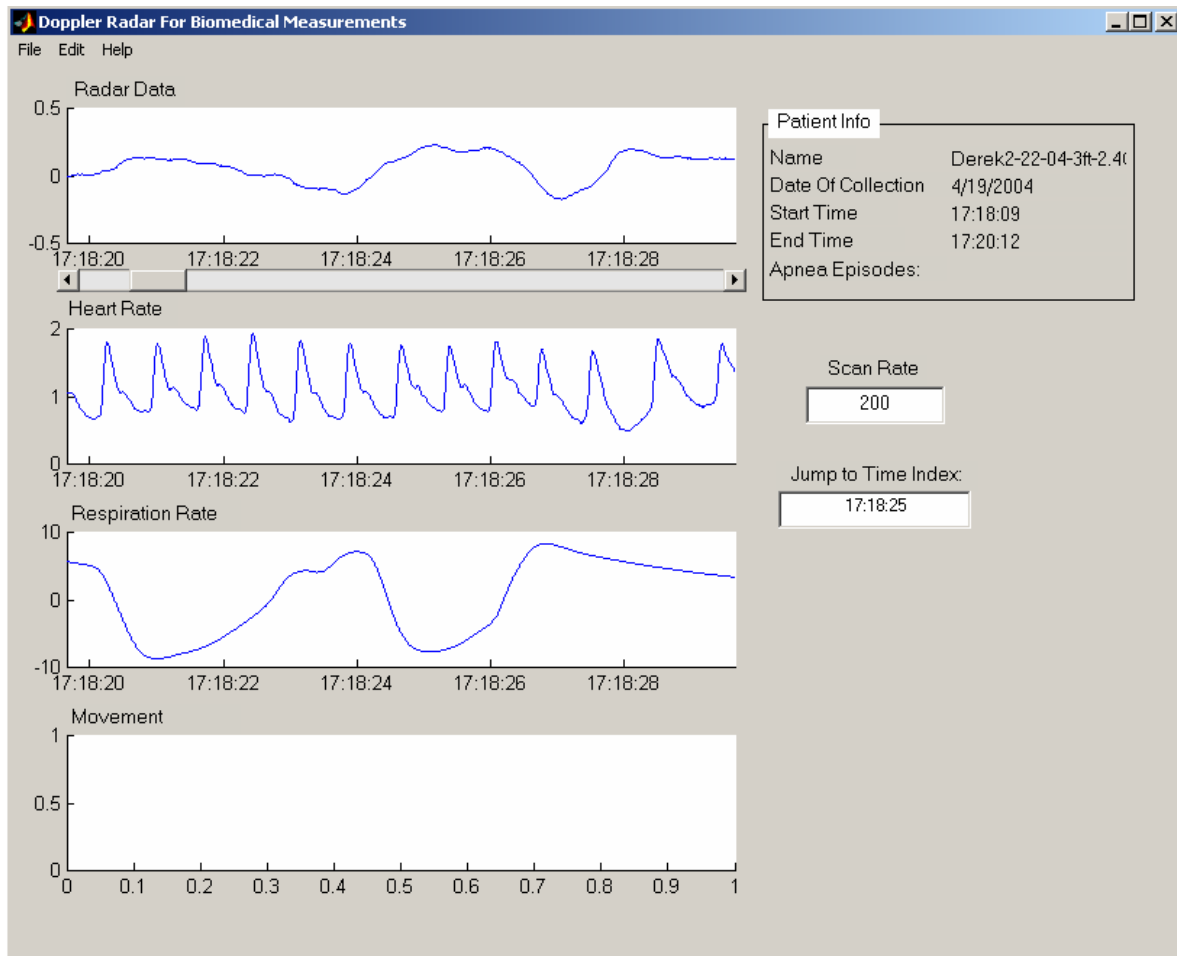


Figure 15 - A Screenshot of the GUI

When using the *Jump To Time Index* box, the user can enter time indices in five manners (where d stands for digit – [0-9]): dd:dd:dd, d:dd:dd, dd:dd, d:dd, or d+.

- Dd:dd:dd or d:dd:dd – This is translated by the GUI to be absolute time. For example, if a dataset begins at 21:00 and the user enters 22:35:00, it would move to 1:35:00 into the data.
- Dd:dd or d:dd – This is translated by the GUI to be absolute time without seconds for data sets longer than one hour, or as only minutes and seconds for data sets within a single hour. For example, if the user enters 15:15 in a data set within an hour, the data moves to h:15:15, where h is the hour in which the data set falls. However, if the data set were longer than an hour, then the GUI would interpret that as 15:15:00 and move there.
- D+ - This is translated by the GUI to mean seconds from the start of the data. If the data started at 1:00:00 and the user entered 350, the GUI would display data at 1:05:50.

If any of these times fall outside the range of the data, then the GUI will move as far towards these times as the data allows.

When displaying data, the GUI automatically adjusts the y-axis of the viewing windows to show the data as large as possible for that window. Because of this, the y-axis of the viewing windows changes every time the data being displayed changes. If the user wishes to stop this behavior, the Freeze Axes menu under the Edit menu holds indicators for all four axes. In addition, the user can Freeze/Unfreeze all four axes at once. When an axis is

frozen, its minimum value stays at the minimum value of the entire dataset, likewise for maximum.

Three additional features incorporated into the GUI are:

- The ability to modify patient information (under the Edit menu) if a mistake is made initially.
- The ability to modify the sampling rate, if it is other than the default 200 Hz. This is done in the *Scan Rate* input box.
- The ability to create Debug logs that are helpful in troubleshooting or modifying the functionality of the GUI.

The Debug Mode of the GUI produces an output file (GUIDebug.txt) which will show the reader what callbacks and subroutines the GUI is in along with any pertinent data about variables in those routines. With access to the debug file and the source code for the GUI, debugging any errors that arise should take much less guesswork than standard debugging.

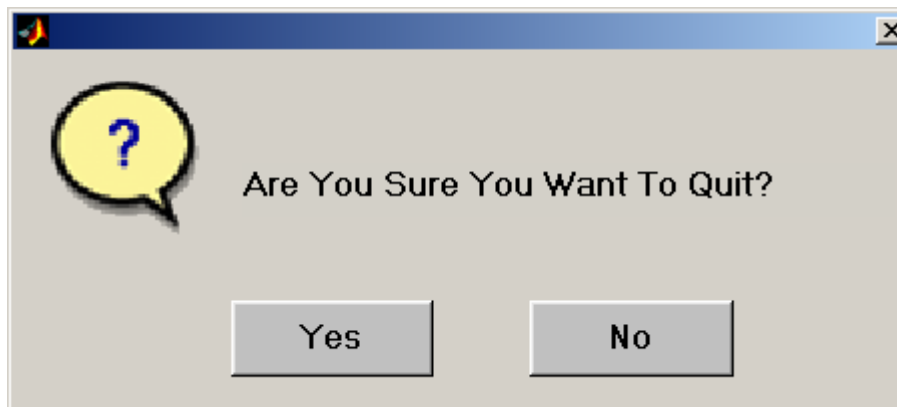


Figure 16 - An Example of User Oversight

In addition, the GUI contains some limited user oversight (program redundancies to prevent a user from losing data). For example, if the user closes a file before saving it, the GUI asks the user if they wish to save the current data set. In Figure 16, the user is asked to confirm if they want to exit the program. If the user enters values incorrectly that the system needs to understand a request (in the *Jump To Time Index* or Patient Information Start Time boxes for example) then the GUI will display an error message. In some cases, the GUI will simply not comply. In these cases, the Debug Mode output file will contain more specific error messages.

Code for the GUI is available in the Digital Appendix CD-ROM.

## 8 Recommendations for Future Work (RS)

The prototype fulfills its intended function but is lacking in the following regards:

- Bulky Hardware and Inconvenient Setup
- Hardware Design Flaw
- Poor Heart Rate Recognition
- Nulls in Range
- Post Processing

### **Bulky Hardware**

The necessary acquisition hardware and PC make this setup impractical. In addition, the AcqKnowledge data acquisition system is much more complex than what is necessary for the application. A smaller and simpler data acquisition system designed for this application would make the system more economical and practical to setup. An ideal feature would be onboard memory to store the night's data for later analysis. In addition, it would be appropriate to develop a stand that can be adjusted in width and height to setup the radar antennas in a person's home for a temporary installation.

### **Hardware Design Flaw**

The potentiometer on the radar boards will short out the power supply when adjusted to zero ohms, since there is no additional resistance in series with the potentiometer to prevent current flow. This causes the monolithic amplifier in the circuit to fail. Two fixed resistors arranged as a voltage divider could provide the target control voltage without the use of the potentiometer in future prototype models. Not only would this eliminate the flaw, but it would also replace the least reliable component present in the prototype and increase the MTTF per unit to 10.88 years, increasing the system MTTF to 21.76 years.

**Poor Heart Rate Recognition**

The heart rate signal is very difficult to locate in the radar data. Noise from surrounding electronics and from drift with the VCO make the characteristic frequency peak nearly impossible to distinguish from noise in the signal. A more accurate VCO and a less noisy environment could make this data more visible.

**Nulls in Range**

When the local oscillator and the received signal are either 0 or 180 degrees out of phase, null points occur. Thus nulls are found with a target distance of  $\lambda/4$  from the radar. With our transmitted frequency of 2.4GHz, these nulls occur every 3cm, which makes them nearly impossible to avoid when monitoring a patient.

A quadrature radar transceiver can eliminate these null spots and would be a valuable improvement on the existing radar hardware. Information on a quadrature receiver designed for vital signs monitoring can be found in the IEEE paper “Range Correlation and I/Q Performance Benefits in Single-Chip Silicon Doppler Radars for Noncontact Cardiopulmonary Monitoring” by Droitcour et al.

**Post Processing**

Post-processing was determined to be acceptable for this application. Should the system be modified to run in real-time however, it could be made substantially more versatile and could be used in applications such as infant monitoring to prevent sudden infant death syndrome.

---

## 9 APPENDICES

<b><u>APPENDIX TITLE</u></b>	<b><u>SECTION</u></b>
References	A
Budget	B
Timeline	C
Reflection and Absorption Supporting Calculations	D
Permittivities and Conductivities of Biological Tissue	E
Interactions of RF Energy and Biological Tissues	F
Breakdown of the Radar Front-End Components	G
Radar Evaluation and Design	H
Digital Appendices	I

---

## 9.1 Appendix A - References

1. <http://www.sleepnet.com/sleepapnea.html>
2. <http://www.lungusa.org/diseases/sleepapnea.html>
3. <http://www.sleepapnea.org/slpapnsk.pdf>
4. <http://www.sleepclinic.org/apnea.html>
5. <http://classes.kumc.edu/cahe/respcared/cybercas/sleepapnea/trenpoly.html>
6. <http://www.talkaboutsleep.com/sleepbasics/viewasleepstudy.html>
7. <http://hyperphysics.phy-astr.gsu.edu/hbase/sound/wavplt.html#c2>
8. Balakrishnan, A. V. Kalman Filtering Theory. New York: Optimization Software, 1987.
9. Baranski, S. and P. Czerski. Biological Effects of Microwaves. Pennsylvania: Dowden, Hutchinson & Ross, 1976.
10. Battocletti, Joseph H. Electromagnetism Man and the Environment. Boulder: Westview Press, 1976.
11. Chen, Kun-Mu, et al. "An X-Band Microwave Life Detection System." IEEE, 1986.
12. Droitcour, Amy, et al. "A Microwave Radio for Doppler Radar Sensing of Vital Signs." IEEE, 2001.
13. Edmonds D. T. Electricity and Magnetism in Biological Systems. New York: Oxford, 2001.
14. Embree, Paul M. and Bruce Kimble. C Language Algorithms for Digital Signal Processing. New Jersey: Prentice Hall, 1991.
15. Johnk, Carl T.A. Engineering Electromagnetic Fields and Waves. New York: John Wiley & Sons, 1988.
16. Lohman, B, et al. "A DSP for Doppler Radar Sensing of Vital Signs." IEEE, 2002.
17. Polk, Charles and Elliot Postow. Handbook of Biological Effects and Electromagnetic Fields. Florida: CRC Press, 1986.

18. Proakis, John G. and Dimitris G. Monolakis. Digital Signal Processing: Principles, Algorithms and Applications. New Jersey: Prentice Hall, 1996.
19. Ramachandra, K.V. Kalman Filtering Techniques for Radar Tracking. New York: Marcel Dekker, 2000.
20. Stearns, Samuel and Ruth A. David. Signal Processing Algorithms in Matlab. New Jersey: Prentice Hall, 1996.
21. Yuen, C.K. and D Fraser. Digital Spectral Analysis. California: CSIRO, 1979.
22. Proakis, John G., Dimitris G. Manolakis. Digital Signal Processing: Principles, Algorithms, and Applications, Third Edition. Prentice Hall, New Jersey. 1996.
23. DeMaw, Doug. Practical RF Design Manual. Prentice-Hall, New Jersey. 1982.
24. Prat, Timothy et al. Satellite Communications. Wiley & Sons. 2003.
25. Droitcour, Amy et al. "Range Correlation and I/Q Performance Benefits in Single-Chip Silicon Doppler Radars for Noncontact Cardiopulmonary Monitoring" IEEE. 2004.
26. [www.radiolab.com](http://www.radiolab.com)

## 9.2 Appendix B – Budget (AB)

The following items were purchased with Biopac funds during our first semester:

<u>Item</u>	<u>Quantity</u>	<u>Cost</u>
VCO 2.4 GHz	2	\$53.90
Amplifier .5-2.5 GHz	6	\$29.70
Mixer 900 MHz	2	\$35.90
VCO 900 MHz	2	\$49.90
Attenuator 12dB	10	\$19.50
Attenuator 15dB	10	\$19.50
Mixer 2.4 GHz	2	\$37.90
Low Pass Filter DC-2.95 GHz	2	\$73.90
Low Pass Filter DC-1 GHz	2	\$25.90
2.4 GHz Antenna	2	\$95.00
SMA plug	3	\$36.12
SMA to BNC plug	3	\$32.73
SMA jack	10	\$44.50
Variable Capacitor .3-1.2 pF	2	\$25.98
Variable Capacitor .8-8 pF	1	\$15.28
<b>Total:</b>	<b>59</b>	<b>\$611.26</b>

---

In addition to these items, we also purchased the following using NMT funds:

<u>Item</u>	<u>Quantity</u>	<u>Cost</u>
ROS-960PV VCO	2	\$19.95
VNA-25 Amplifier	4	\$4.70
RMS-5H Mixer	2	\$16.85
BLP-150 LP Filter	2	\$32.95
Parts Bin	1	\$12.00
Tin Foil	1	\$3.00
Freight Charges		\$38.49
Total:	8	\$211.79

We also received 5 additional LAT-12 attenuators from Minicircuits, and three variable capacitors from Mouser Electronics free of charge.

### 9.3 Appendix C - Project Timeline (DL)

Task	Date		Manpower Hours
	Start	End	
<b>Documentation</b>			
Statement of Work	10/01/03		60
Preparation for Conceptual Design Review	10/01/03	10/07/03	60
Conceptual Design Review	10/07/03		
Preparation for Preliminary Design Review	10/07/03	10/21/03	60
Preliminary Design Review	10/21/03		
Preparation for Critical Design Review	10/21/03	11/04/03	60
Critical Design Review	11/04/03		
Write Formal Report	11/15/03	12/03/03	120
Formal Report	12/03/03		
Preparation for Thesis	03/15/04	04/20/04	120
Thesis	04/20/04		
Thesis Presentation Preparation	04/20/04	04/30/04	
Thesis Presentation	04/30/04		
<b>Doppler Front End</b>			
Consult w/ Dr. Scott on Existing Designs	13/03/03		8
Training w/ Alan Macy and Dr. Scott	10/09/03		8
Purchase 2.5 GHz Prototype Supplies	10/09/03		20
Evaluate 1900 Mhz Unit	10/10/03	11/04/03	20
Evaluate 900 MHz Unit	10/10/03	11/04/03	20
Investigate Antenna Design	10/10/03	11/03/03	40
Investigate Antenna Purchase Options	10/10/03	11/01/03	40
Determine Conceptual Antenna Design	11/04/03		
Refine Antenna Array Design	11/04/03	12/02/03	20
Determine Final Array Configuration	12/03/03		
Build 2.5GHz Prototypes and 900MHz Prototypes	12/04/03	12/23/03	40
Build Antenna Mounting Hardware	12/04/03	12/23/03	2
Test Antenna Array Design	12/26/03	01/07/03	20
Collect Small Apnea Data Sets	02/27/04		2
Collect Abnormal Data Sets	02/27/04		10
Collect Movement Data Sets	02/27/04		2
Collect Long Apnea Data Sets	03/19/04		6
Collect Long Sleeping Data Sets	03/19/04		6

Task	Date		Manpower Hours
	Start	End	
<b>DSP Engine</b>			
Investigate Existing Techniques and Methods	10/10/03	12/03/03	40
Evaluate DSP engine with new 2.5 GHz Front End	11/20/03	11/25/03	20
Determine needed DSP Engine Specs	11/02/03		60
Determine Hardware or Software Implementation	11/02/03		10
Determine Preliminary Design	11/02/03	12/03/03	60
Programming Initial Single Antenna Program	12/03/03	01/07/04	100
Develop Respiration Algorithm	03/01/04		40
Test Respiration Algorithm	03/02/04	03/19/04	10
Develop Heart Rate Algorithm	03/01/04	03/19/04	40
Test Heart Rate Algorithm	03/19/04	04/20/04	10
Develop Movement Algorithm	03/19/04	04/14/04	20
Test Movement Algorithm	04/14/04	04/20/04	10
Develop Apnea Algorithm	03/19/04	04/19/04	20
Test Apnea Algorithm	04/19/04	04/20/04	10
<b>GUI System</b>			
Investigate Existing Techniques and Methods	10/10/03	11/02/03	40
Evaluate Existing GUI	10/10/03	11/02/03	20
Determine needed GUI Specs	11/02/03		
Determine Redesign or Modification	11/02/03		
Determine Preliminary Design	11/02/03	12/03/03	20
Preliminary Front End Done	12/03/03	03/22/04	80
Final Front End Done	03/22/04	04/20/04	100
Back End Development	03/22/04	04/20/04	100
Back End Complete	04/20/04		
<b>System Integration</b>			
Incorporate GUI, DSP Engine and Radar	02/01/04	02/20/04	40
Prototype Finished	04/01/04	04/20/04	
Deliver Prototype	05/01/04	04/30/04	

## 9.4 Appendix D - Reflection and Absorption Supporting Calculations (KS)

The complex amplitude of the reflected wave

Intrinsic wave impedance of free space

$$\hat{\eta}_1 = \sqrt{\frac{\mu}{\epsilon - j\frac{\sigma}{\omega}}} = \sqrt{\frac{4\pi \times 10^{-7}}{\frac{10^{-9}}{36\pi} - j\frac{0}{2\pi(2.5 \times 10^9)}}} = \sqrt{\frac{(4\pi \times 10^{-7})}{\frac{10^{-9}}{36\pi}}} = \sqrt{142122} \cong 377$$

Intrinsic impedance of skin

$$\begin{aligned} \hat{\eta}_2 &= \sqrt{\frac{\mu}{\epsilon - j\frac{\sigma}{\omega}}} = \sqrt{\frac{4\pi \times 10^{-7}}{(33 \times \frac{10^{-9}}{36\pi}) - j\frac{1}{2\pi(2.5 \times 10^9)}}} = \sqrt{\frac{4\pi \times 10^{-7}}{2.92 \times 10^{-10} - j1.59 \times 10^{-10}}} \\ &= \sqrt{\frac{(4\pi \times 10^{-7})(2.92 \times 10^{-10} + j1.59 \times 10^{-10})}{(2.92 \times 10^{-10} - j1.59 \times 10^{-10})(2.92 \times 10^{-10} + j1.59 \times 10^{-10})}} = \sqrt{\frac{(3.67 \times 10^{-16} + j1.998 \times 10^{-16})}{(8.526 \times 10^{-20} - 2.53 \times 10^{-20})}} \\ &= \sqrt{3.321 \times 10^3 + j1.8 \times 10^3} \end{aligned}$$

$$(a + jb)^{\frac{1}{2}} = r^{\frac{1}{2}} e^{j\frac{1}{2}\theta}$$

$$r = \sqrt{1.1 \times 10^7 + 3.24 \times 10^6} = \sqrt{1.42 \times 10^7} = 3.77 \times 10^3$$

$$\theta = \tan^{-1}\left(\frac{-3.24 \times 10^6}{1.1 \times 10^7}\right) = \tan^{-1}(-2.945 \times 10^{-1}) = -16.41$$

Polar Form

$$\hat{\eta}_2 = (3.77 \times 10^3)^{\frac{1}{2}} e^{j\frac{1}{2}(-16.41)} = 61.4 e^{j8.205}$$

Trigonometric Form

$$\hat{\eta}_2 = 61.4e^{j8.205} = 61.4(\cos(-8.205) + j\sin(-8.205)) = 61.4(0.989 + j(-0.143))$$

$$= 60.72 - j8.76$$

$$\frac{\hat{\eta}_2 - \hat{\eta}_1}{\hat{\eta}_2 + \hat{\eta}_1} = \frac{60.72 - j8.76 - 377}{60.72 - j8.76 + 377} = \frac{-316.28 - j8.76}{437.72 - j8.76} = \frac{(-316.28 - j8.76)(437.72 + j8.76)}{(437.72 - j8.76)(437.72 + j8.76)}$$

$$= \frac{-138422 - j2770.6 - j3834.42 + 76.737}{191598.8 + 76.737} = \frac{-138345 - j6605}{191675.5} = -0.72 - j0.0344$$

Therefore the calculation below shows around 72% of energy will be reflected back.

$$\hat{E}_{m1}^- = \hat{E}_{m1}^+(-0.72 - j0.0344)$$

## 9.5 Appendix E - Permittivity and Conductivity of Biological Tissue as a Function of Frequency

Frequency	Conductivity (S/m)										
	A	B	C	D	E	F	G	H	I	J	K
	Skeletal muscle parallel	Skeletal muscle perpendicular (nonoriented)	Liver	Lung	Spleen	Kidney	Brain white matter	Brain grey matter	Bone	Whole blood	Fat
1 } 10 Hz	0.52	0.076	0.12	0.089							
2 } 10 Hz											
3 } 10 Hz											
4 } 100 Hz	0.52	0.076	0.13	0.092					0.0126	0.60	
5 } 100 Hz											
6 } 100 Hz											
7 } 1 kHz	0.52	0.08	0.13	0.096					0.0129	0.68	0.02-0.07
8 } 1 kHz											
9 } 1 kHz											
10 } 10 kHz	0.55	0.085	0.15	0.11					0.0133	0.68	
11 } 10 kHz											
12 } 10 kHz											
13 } 100 kHz	0.65	0.40	0.15	0.62		0.24-0.25	0.12-0.15	0.17	0.0144	0.55	
14 } 100 kHz	0.56-0.59		0.16							0.68	
15 } 100 kHz	0.38-0.44										
16 } 1 MHz	0.83-0.85		0.27	0.63		0.37-0.39	0.14-0.19	0.21	0.0173	0.71	
17 } 1 MHz	0.58-0.63		0.30								
18 } 1 MHz	0.86-0.87		0.47	0.84		0.64-0.68	0.21-0.28	0.35	0.0237		
19 } 10 MHz	0.92-0.96		0.46	0.55-0.53		0.50-0.57	0.30	0.38		1.11	
20 } 10 MHz	0.69-0.75		0.42-0.46				0.29-0.31	0.45-0.63			
21 } 10 MHz	0.95-0.99		0.72	1.05		0.94-1.05	0.36-0.48	0.69	0.0574	1.0	0.02-0.07
22 } 100 MHz	0.9 ± 0.08		0.70	0.73-0.76		0.66-0.72	0.45	0.7			
23 } 100 MHz	0.75-0.82		0.60-0.71	1.2		0.75 ± 0.02	0.48-0.51	0.52-0.85		0.7-0.8	
24 } 100 MHz	1.38-1.45		0.98	0.80 ± 0.02			0.89-0.94		0.05	1.4-1.6	
25 } 1 GHz	1.3		1.2	1.2		0.95-0.97	0.80	1.1		1.3	0.03-0.09
26 } 1 GHz	1.5		0.95-1.0	2.0		1.0	0.81-0.82	0.89-1.17			
27 } 1 GHz			2.0	2.5 ± 0.03			1.8-2.1		0.16	2.5-3.1	
28 } 3 GHz	2.7 ± 0.07		2.4	2.7		2.3 ± 0.05	1.5	2.0			
29 } 3 GHz	2.8		2.8								
30 } 3 GHz											

		Relative Permittivity									
31 } 10 GHz	8.3	5.8—6.7	6.5	10	0.5—1.7	9.1	0.3—0.4				
	32 } 7.7	10.0	10.0	8	10.5	10.5					
	33 } 8.8										
1 } 10 Hz	10 <sup>7</sup>	5 × 10 <sup>7</sup>	2.5 × 10 <sup>7</sup>								
2 } 10 Hz											
3 } 100 Hz	1.1 × 10 <sup>6</sup>	3.2 × 10 <sup>5</sup>	4.5 × 10 <sup>5</sup>		3,800	1.5 × 10 <sup>5</sup>					
4 } 100 Hz											
5 } 1 kHz	2.2 × 10 <sup>5</sup>	1.2 × 10 <sup>5</sup>	8.5 × 10 <sup>4</sup>		1,000	5 × 10 <sup>4</sup>					
6 } 1 kHz											
7 } 1 kHz											
8 } 10 kHz	8 × 10 <sup>4</sup>	7 × 10 <sup>4</sup>	2.5 × 10 <sup>4</sup>		640	2 × 10 <sup>4</sup>					
9 } 10 kHz											
10 } 10 kHz											
11 } 10 kHz											
12 } 10 kHz	1.5 × 10 <sup>4</sup>	3 × 10 <sup>4</sup>			280						
13 } 100 kHz											
14 } 100 kHz	24,800—27,300	9,760	3,260	10,900—12,500	1,960—3,400	3,800					
15 } 100 kHz	14,400—15,800	1.4 × 10 <sup>4</sup>									
16 } 1 MHz	1,970	1,970	1,450	2,390—2,690	543—827	1,250					
17 } 1 MHz	2,460—2,530										
18 } 1 MHz	1,900—2,150										
19 } 10 MHz	170—190	338	321	431—499	163—209	352					
20 } 10 MHz	187—204	300	352—410	190—204	200	380					
21 } 10 MHz	162—181	251—265			190—191	237—289					
22 } 100 MHz	67—72	77	83	89—95	57—66	90					
23 } 100 MHz	68 ± 2	79	35	56—62	65	90					
24 } 100 MHz	64—70	65—68		85 ± 1	58—64	65—80					
25 } 1 GHz	57—59	46	54	43	40—44	45					
26 } 1 GHz	58	55	50—51	46	35	45					
27 } 1 GHz	48	47—49	50	38—39	38—39	47—51					
28 } 3 GHz		42	52.0.6	35—41	35—41	44					
29 } 3 GHz	52.5 ± 0.7	53									
30 } 3 GHz	46	42—43	46	47.5 ± 1							
31 } 10 GHz	40—42	34—38	42								
32 } 10 GHz	37	37	38	30—37	25	40					
33 } 10 GHz	35										

---

## 9.6 Appendix F - Interactions of RF Energy and Biological Tissues (DL)

This section will give a brief introduction into the theory of boundary conditions of a traveling RF wave hitting the various tissue types of the body. Also explored are the permeability and conductivity of said tissues.

When thinking about interactions between electromagnetic waves and biological tissue, the concepts are no different than considering the interactions between a wave of any frequency and a boundary and material of any conductivity, permeability, and permittivity. In all types of body tissue, magnetic permeability is very closely equal to  $\mu_0$ , or the permeability of free space. This fact makes most calculations involving body tissues simpler. The more important concepts to consider at the frequencies the prototype will operate at (900MHz and 2.4GHz) are the reflectivity coefficients and skin depth of penetration, because from these, energy absorption and the distribution of energy can be derived. While the specifics of energy distribution inside a tissue is rather complex and beyond the scope of our research, we are still interested in net energy (and thus power) absorption to determine if our power output will be within OSHA-defined limits.

It is worthwhile to note that for the antennas to be used, and at the frequencies transmitted, all occurrences will happen in the far-field region of the antenna. The far-field region is defined as the region of space, a minimum distance  $l$  from the emitting antenna to infinite, that the transmitted energy waves can be seen as a predominantly plane-wave character (electric vector  $\mathbf{E}$  is perpendicular to the  $\mathbf{H}$ -field vector) [17]. The

region of operation for our device, 0.5 m at the closest to 2m, nearly assures operation in the far-field region of the antennas, which is defined by the equation [17]:

$$l = \frac{2D^2}{\lambda}$$

Where D is the larger dimension of the antenna and with wavelength  $\lambda$  as defined by [15]:

$$\lambda = \frac{V_{prop}}{f} \qquad V_{prop} = \frac{c}{\sqrt{\epsilon_R}}$$

Wavelengths  $\lambda$  for the frequencies of our devices are 33 cm, for 900MHz, and 12.5 cm, for 2.4GHz. These yield far-field regions beginning at 27 cm (D = 20.32 cm) and 16 cm (D = 10.8 cm), respectively. The fact that the prototypes will be operating in the far-field region assures simpler power calculations and considerations: the power density travels as one over the square of the distance traveled in the far-region (as opposed to having to calculate the more complex oscillations that characterize power transmission in the near field) [17].

When the near-planar wave of energy hits the body tissue, the system acts as a typical wave hitting a boundary with different characteristics than the current medium. In this case, the wave traveling in free space (air) contacts the skin of the patient. As with any such interaction, part the wave is reflected back to the source while the remnant is transmitted into the skin. The reflection coefficient that defines what is reflected back is dependent upon the frequency of the wave, the permeability, conductivity, and permittivity of both sides of the boundary. Its value is determined by using a ratio of the

pre- and post-boundary impedances defined by the aforementioned characteristics. A discussion of the coefficient can be found in the CRC Handbook of Biological Effects of Electromagnetic Fields [17], pages 14-15. The governing equation is found below:

$$\Gamma = \frac{\eta_2 - \eta_1}{\eta_2 + \eta_1}$$

Where  $\Gamma$  is the reflection coefficient and  $\eta$  is the wave impedance of medium 1 and 2.

Continuing the discussion of the air-to-skin transmission, the transmitted wave inside the boundary will continue to penetrate the body, but it will attenuate at an exponential rate, dependent on the skin depth of the material<sup>17</sup>. The skin depth  $\delta$  is also a function dependent on the medium's permittivity, permeability, and conductivity, as well as the wave's frequency. Refer to the CRC Handbook of Biological Effects of Electromagnetic Fields [17] for a discussion and the governing equations for transmission attenuation and skin depth calculation. Here is a table of calculated skin depths for various tissues at various frequencies. Frequencies of interest are the 915 MHz and the 2450MHz rows. Follows is the equation that governs skin depth for all materials:

$$\delta = \frac{1}{\omega \sqrt{\frac{\mu\epsilon}{2} \left( -1 + \sqrt{1 + \frac{\sigma}{\omega\epsilon}} \right)}}$$

**DEPTH OF PENETRATION OF AN  
ELECTROMAGNETIC WAVE IN  
BIOLOGICAL TISSUES AS A FUNCTION OF  
FREQUENCY**

Frequency (MHz)	Tissue				
	Saline	Blood	Muscle (skin)	Lung	Fat (bone)
	<b>Depth of Penetration (cm)</b>				
433	2.8	3.7	3.0	4.7	16.3
915	2.5	3.0	2.5	4.5	12.8
2,450	1.3	1.9	1.7	2.3	7.9
5,800	0.7	0.7	0.8	0.7	4.7
10,000	0.2	0.3	0.3	0.3	2.5

**Figure 17 - Skin Depth as a Function of Frequency**

The human body of course does not consist of a homogenous material (single tissue) with a single boundary at the skin. Each tissue has its own permittivity and conductivity characteristics. The biology of this is interesting, but only worth a cursory mention; factors such as the average water content of a tissue, cell size and shape, intra- and extra-cellular ion concentration, and plasma membrane structure play a part in defining the cell's characteristics. A table of the conductivities and permittivities of the various tissues can be found in Appendix E. These properties are noticeably different from tissue to tissue and warrant calculations for each transition.

Because of this heterogeneity, numerous different boundaries must be considered; for example, the path between the skin and the heart has layers of fat, muscle, bone and cartilage, all in varying amounts, depending on the patient. The calculations to do this are too elaborate to examine here; Chapter 6 in Engineering Electromagnetic Fields and Waves contains the procedure for considering multiple heterogeneous regions.

At the frequencies that the prototypes will be operating at, the penetration (and thus power dispersal) the majority of the transmitted energy is absorbed as the attenuating wave passes through the body. After this point, most of the power will have either been reflected back or absorbed by the tissues through which the wave has propagated (with the minimal remaining amounts of energy continuing on). Thus, the tissues of concern are the focus of safety considerations. The OSHA standard limit for continuous exposure for the frequencies of our operation is  $10 \text{ W/cm}^2$ . Other organizations also release comparable recommendations for legal limits; ANSI (American National Standards Institute) and IEEE release their own limits, with the former being stricter than the latter, whose values parallel the OSHA standards. While the power output for the range of our prototypes have not yet been measured, the designer of the circuitry estimates that the power output of the antennas are well below this limit. This is beneficial, because if the resulting data is not discernable, we will be able to increase our output power to receive signals back with higher amplitude.

## 9.7 Appendix G - Breakdown of the Major Radar Front-End Components (KS)

### Mixer

There are two signals that are compared by the mixer. One is from the local oscillator (the VCO) and is referred to as LO. The second is the reflected signal that comes from the RF antenna and is appropriately referred to as the RF. If we represent LO as  $\cos \omega_1 t$  and RF as  $\cos \omega_2 t$ , we can evaluate their relationship in the mixer as

follows:  $(\cos \omega_1 t)(\cos \omega_2 t)$ .

A circuit diagram demonstrating how this relationship is achieved is shown below:

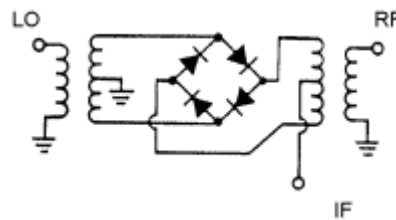


Figure 18 - LO Circuit Equivalence

As you can see from the circuit, a certain level of power is required on the LO input to properly driver the mixer diodes. LO power level has to be sufficient in order to turn on the diode in the saturation mode. The LO power level must also be much larger than the RF power level in order to prevent load distortion. The LO drive level plays a critical role in determining the  $IP^3$ , 1 dB Compression Point and Dynamic Range of a mixer. For higher performance applications, Pulsar recommends as a minimum the use of a +17 dBm level mixer.

## Voltage Control Oscillator

A fundamental oscillator circuit is shown in Figure 19.

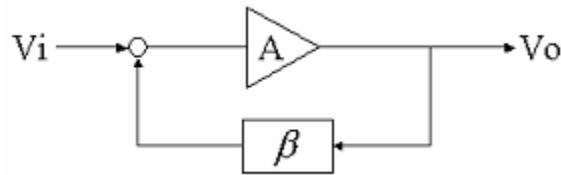


Figure 19 - Fundamental Oscillator Circuit Representation

In order to oscillate, the total phase shift of this closed loop has to be 360 degrees and the

gain must be one:  $\frac{V_o}{V_i} = \frac{A}{(1 - \beta A)}$  In our project, we used a 2.4GHz oscillator.

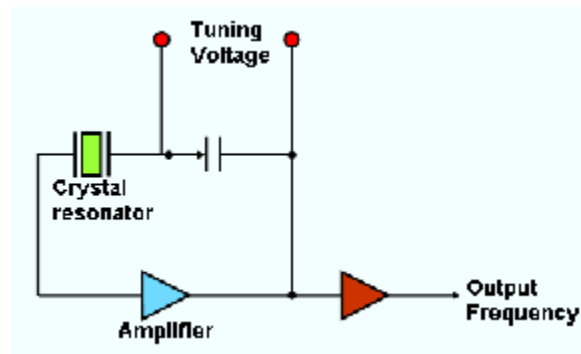


Figure 20 - VCO Representation

Figure 20 is the common configuration of the crystal oscillator. Most oscillators operate

at “parallel resonance” where the reactance vs. frequency slope,  $\frac{dx}{df}$ , is inversely

proportional to  $C_1$ , the motional capacitance of the crystal unit. The principal

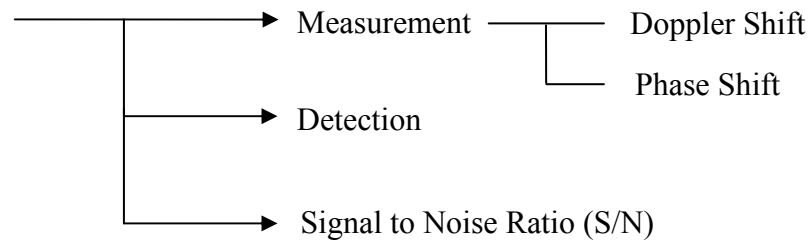
mechanism of the voltage-controlled oscillator is that the circuit is only marginally stable.

Thus the output of the system oscillates at the constant amplitude and frequency.

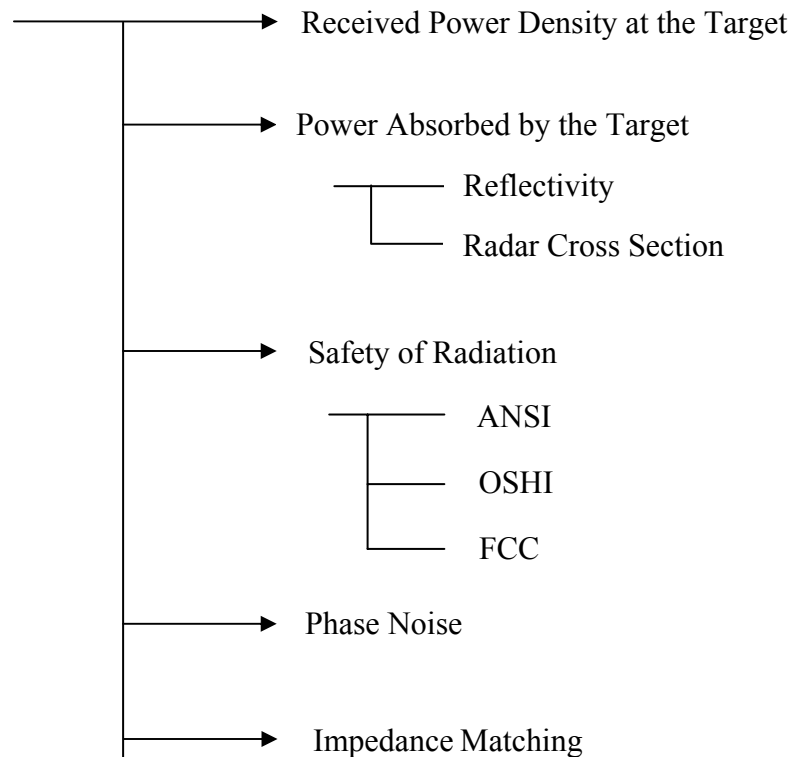
## 9.8 Appendix H – Radar Evaluation and Design (KS)

In this section we will introduce some concepts that would have been necessary in the full design of a radar system. The design flow and power are discussed in the flow chart below:

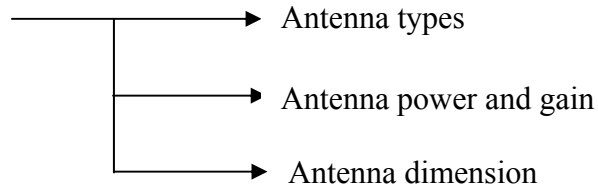
1. Determination of adequate signal and frequency which can provide sufficient information of the target.



2. Power calculation at the transmitter, receiver, and target.

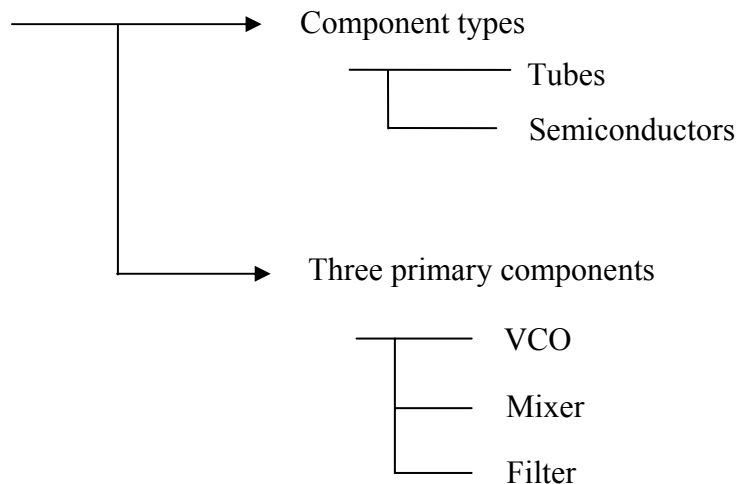


3. According to the information above, choose antenna types and specifications.



Based on the desired power density, the antenna specifications such as antenna type, gain, dimensions and power can be determined.

4. Fundamental RF circuit design and analysis



### Determination of adequate signal and frequency

Higher frequency operation (shorter wavelength) can make the antenna size smaller. It can also increase the range of the unit and make any phase changes more distinguishable.

When designing a Doppler radar, we need to determine if the target moves fast enough to give us a Doppler shift. If not, a phase detector type application is the alternative. Actual received power at the antenna is obtained by the following equation:

$$P_r = \frac{P_t G_t G_r \lambda^2}{(4\pi)^3 R^4} \sigma$$

### Signal to Noise Ratio (S/N)

The signal-to-noise ratio needs to be considered at this stage. The S/N ratio shows can be used to determine how difficult it will be to extract the desired signal from the noise present in the system. The noise is defined as  $N=kTB$ , where  $k$  is the Boltzmann's constant (-228.6dBW),  $T$  is temperature, and  $B$  is the noise bandwidth.

Combining two equations gives us the S/N ratio expressed as follows:

$$\frac{S}{N} = \frac{P_t G_t G_r \lambda^2}{(4\pi)^3 R^4 kTB} \sigma$$

A signal-to-noise ratio of greater than 10dB is the typical way to set up these system's efficiency.

### Power calculation at the transmitter, receiver, and target

The power density at the target is obtained from following equation:

$$P_r = \frac{P_t G_t G_r \lambda^2}{(4\pi)^2 R^2}$$

$P_t = -20\text{dB}(10\text{dBm})$ ,  $G_r = G_t = 8\text{dB}(8\text{dBi})$ ,

The parameters are divided to the numerator and denominator. After converted into dB, the parameters which are listed in the numerator are simply added and the parameters on the denominator are subtracted. Knowing this figure, one can adjust the power

transmitted and received to determine if sufficient signal strength is available at the RF input of the mixer. This is discussed in greater detail in Appendix G.

### Phase Noise

In order to obtain the highest functionality of the system, typical signal distortion such as phase noise or “jitter” needs to be considered. Let say that a perfect VCO would produce an ideal sine wave:

$$V(t) = A \sin(\omega t)$$

However, there is inherently some noise introduced to the signal. This can be represented by fluctuations in the amplitude of the signal and by fluctuations in the signal phase. We can represent the noisy oscillator signal as:

$$V(t) = (A + a(t)) \sin(2\pi f_o t + \phi(t))$$

where  $a(t)$  represents the amplitude noise and  $\phi(t)$  represents the phase noise.

Amplitude noise can be removed to some degree by using automatic level control (ALC) systems. However, phase noise is another matter. It is very difficult to remove.

The equation can be rewritten ignoring amplitude noise:

$$V(t) = A \sin(2\pi f_o t + \phi(t))$$

The picture below shows the effect of  $\phi(t)$ .

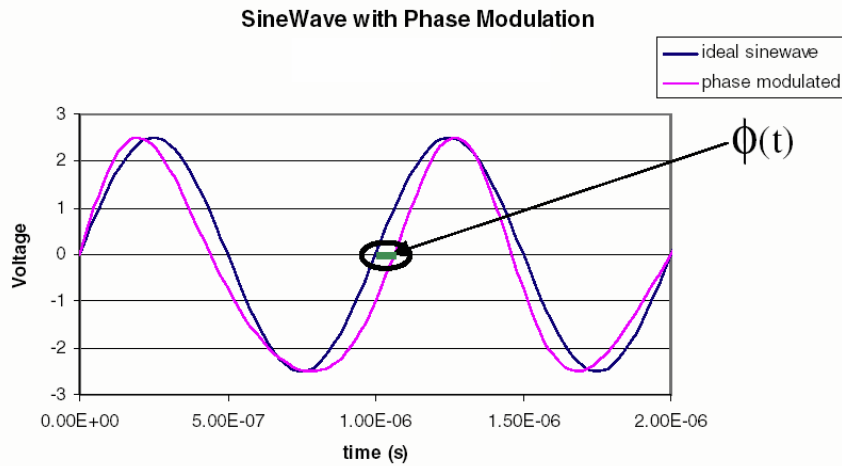


**Figure 21 - Phase Noise Diagram**

Phase noise is a serious source of interference, such as “timing error” in the RF design. Especially in our system, which obtains information from the phase shift measurement.

“Minute amounts of phase noise on a transmitter signal can result in the transmitter causing significant interference to other services, whereas minute amounts of phase noise on a receiver local oscillator can severely reduce the receiver selectivity or cause other undesirable effects.” [26] Minimizing phase noise is one of most important factors in the selection of a VCO and is frequently a selling point in the VCO spec sheet.

### **Impedance Matching**

Impedance matching is another important aspect of RF circuit design. Matching the source impedance and the load impedance produces maximum output power and avoids creating standing waves. A mismatch caused by these can result in interference when they add or subtract signals on the transmission line. This is avoided by careful design

during the board etching process. Our boards were professionally designed and etched by MiniCircuits.

### Antenna Types

There are many different types of antennas: a few examples are helix, yagi, and patch antennas. Patch antennas are employed in our project because of their small size, but yagi antennas were very appealing due to their increased directionality.

### Antenna Dimension

It is appropriate to compare the antenna's dimensions with the size of the wavelength instead of just evaluating its physical size. For instance, a 30m high AM antenna is small in terms of its wavelength, which is 300m. One advantage of using microwave frequency bands is that the wavelengths (and thus the antennas) are rather small. In our project, the antenna has a physical size of 9.9cm x 10.7cm. This is efficient when we consider the wavelength, which is 12.5cm.

Antenna gain can be obtained by the following equation:

$$G = \eta_A \frac{4\pi A}{\lambda^2} = \eta_A \left( \frac{\pi D}{\lambda} \right)^2$$

Antenna gain is proportionally related to the area (A) of the antenna and inversely proportional to the wavelength. For this project, one reason why the 2.4GHz band was selected was the smaller antenna size. From the above equation above, the antenna efficiency,  $\eta_A$  also can be determined as follows:

$$\eta_A = \frac{G_t \lambda^2}{4\pi A} = 0.7311$$

## 9.9 Digital Appendices

The following files are available on the CD-ROM:

- Executable File
- Source Code
- Sample Data Sets
- User Manual